

Needle-less Injection System for Drug Delivery

by

Robert Joseph Dyer

B.S., Mechanical Engineering (2001)

Massachusetts Institute of Technology

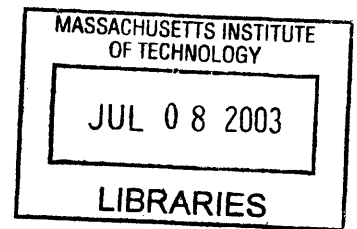
Submitted to the Department of Mechanical Engineering in
Partial Fulfillment of the Requirements for the Degree of

Master of Science in Mechanical Engineering

at the

MASSACHUSETTS INSTITUTE OF TECHNOLOGY

[Stamp: JUL 08 2003]
February 2003



© 2003 Massachusetts Institute of Technology. All rights reserved.

Signature of

Author:.....

~~Department of Mechanical Engineering~~
January 17, 2003

Certified

by:.....

Ian W. Hunter
Professor of Mechanical Engineering and Professor of BioEngineering
Thesis Supervisor

Accepted

by:.....

[Signature]
Ain A. Sonin
Professor of Mechanical Engineering
Chairman, Department Committee on Graduate Students

Needle-less Injection System for Drug Delivery

by

ROBERT JOSEPH DYER

Submitted to the Department of Mechanical Engineering
on January 17, 2003 in partial fulfillment of the
requirements for the Degree of Master of Science in
Mechanical Engineering

Abstract

A needle-less injection device is capable of delivering a liquid drug through skin tissue via a high-speed stream. Devices currently on the market use compressed gas to provide the necessary drug pressure. Shape memory alloy, due to its ability to generate high stresses and its contractile properties, has recently been proposed as a method of actuation for a needle-less injection system. A proof of concept model described here injects, with marginal success, into pig skin tissue to depths of 2 mm and at volumes of up to 200 μL . The diameter of the fluid stream was 150 μm . This device uses six 380 μm NiTi wires around the 150 mm long central body to contract a 6 mm piston a distance of 7 mm. Contraction of the NiTi wires was done by joule heating from current supplied by a 50 V 0.156 F capacitor bank. Further injection tests were conducting with a second prototype having eight NiTi wires on the body and a variable drug volume. Measurements of energy dissipation, piston position, drug injection speed and injection success were conducted using several interchangeable modules. Drug vials ranged in volume from 20 μL to 500 μL with an orifice size of 100 μm . It was found that injections of 20 μL penetrated the tissue to depths of 10 mm while volumes of 250 μL only penetrated 1 mm and 500 μL drug vials had no injection success. Measured drug speeds for the 20 μL and 250 μL volumes reached 160 m/s and 65 m/s respectively. Energy dissipation during typical successful 15 ms injections was approximately 60 J. Tests from the second prototype show that drug vial diameters from 3mm to 5 mm have the most promise for successful injections.

Thesis Supervisor: Ian W. Hunter

Title: Professor of Mechanical Engineering and Professor of BioEngineering

Acknowledgments

I would like to thank Professor Ian Hunter for the privilege of working in the Bio-Instrumentation Lab. It has been an amazing experience which I will never forget. I would also like to thank Norwood Abbey for funding the needle-less injection project which I enjoyed working on for a year and a half. I would have never been introduced to the Bio-Instrumentation Lab if it was not for Sylvan Martel who took me on as UROP as an undergraduate.

Kara Meredith has been one of my biggest supporters through out this process and has stuck by me even though we have been separated for so long. I would like to especially thank her for all her help with this document; especially the proof reading.

I would like to thank all the people I have known and worked with in the Bio-Instrumentation Laboratory for making it a great place to work. There are some people I would especially like to recognize for their efforts in helping me with this document. Bryan Crane and Peter Madden worked many hours proof reading my thesis and have helped me to make it much better.

Finally I would like to thank my family who is always supportive of me in whatever I do. My parents were the first people to introduce me to engineering, giving up many hours to help me with all of my projects.

Table of Contents

ABSTRACT	3
ACKNOWLEDGMENTS	4
LIST OF FIGURES	8
LIST OF TABLES	10
1 INTRODUCTION	11
2 BACKGROUND	12
2.1 NEEDLE-LESS INJECTION	12
2.2 SHAPE MEMORY ALLOY	15
3 OVERALL DEVICE REQUIREMENTS	19
4 FEASIBILITY ANALYSIS	20
4.1 REQUIRED PRESSURE AND FLUID RATE ANALYSIS	21
4.1.1 Pressure requirement	21
4.1.2 Drug injection rate	22
4.2 ENERGY REQUIREMENTS	22
4.3 SIZE REQUIREMENTS	23
5 PROTOTYPE 1 DESIGN	24
5.1 PROTOTYPE DESIGN GOALS	24
5.2 PROTOTYPE 1 DESIGN CONSIDERATIONS	24
5.2.1 Structure	24
5.2.2 Actuation	25
5.2.3 Critical dimensions	25
5.2.4 Criteria	25
5.3 PROTOTYPE DESIGN	26
5.3.1 Overall device	26
5.3.2 Nozzle	28
5.3.3 Piston Cylinder	34
5.3.4 NiTi actuator	39
5.3.5 Power Source	40
5.4 PROTOTYPE 1 TESTING AND ANALYSIS	42
5.4.1 Injection Test	42
5.4.2 Discharge test	45
5.5 PROTOTYPE 1 DESIGN ANALYSIS	46

5.6	TESTING CONCLUSIONS	46
5.7	DESIGN REQUIREMENTS CONCLUSIONS	47
5.8	NOTES FOR FURTHER REVISIONS	47
6	PROTOTYPE 2	48
6.1	PROTOTYPE 2 DESIGN GOALS	48
6.2	DESIGN CRITERIA FOR PROTOTYPE 2	49
6.3	COMPONENTS	51
6.4	INJECTION DEVICE.....	51
6.4.1	<i>Overview of basic layout</i>	51
6.4.2	<i>Body</i>	52
6.4.3	<i>Pusher</i>	53
6.4.4	<i>Drug Vial</i>	54
6.4.5	<i>NiTi wire</i>	56
6.5	TESTING COMPONENTS	57
6.5.1	<i>Voltage and current</i>	57
6.5.2	<i>Skin Force Measurement</i>	58
6.5.3	<i>Drug vial position measurement</i>	59
6.5.4	<i>Drug Velocity</i>	61
6.5.5	<i>Drug pressure velocity measurement</i>	64
6.5.6	<i>Setup Housing</i>	66
6.6	TESTING AND DATA	67
6.6.1	<i>Injection test</i>	67
6.6.2	<i>Drug Velocity</i>	72
6.6.3	<i>Pressure Velocity measurements</i>	74
6.7	TEST MEASUREMENT ANALYSIS	75
7	CONCLUSION	76
8	FURTHER RESEARCH.....	76
8.1	PROTOTYPE 2.....	76
8.2	STRAIN RATE MEASUREMENTS.....	77
8.3	FURTHER RESEARCH PROTOTYPES	77
	REFERENCES.....	78
	APPENDIX A	80
	FEASIBILITY ANALYSIS	80
	APPENDIX B	82

TURBULENT FLOW ANALYSIS82

APPENDIX C83

 PRESSURE DROP AROUND PLUNGER.....83

 HOOP STRESS CALCULATIONS84

APPENDIX D85

 POWER SUPPLY CIRCUIT85

APPENDIX E86

 PROTOTYPE 2 INJECTION PHOTOGRAPHS86

List of Figures

<i>Figure 2-1. Injection method for needle-less injection systems.</i>	12
<i>Figure 2-2. Size comparison of a human hair, 24 gauge needle and drug stream.</i>	13
<i>Figure 2-3. Basic components of most needle-less injection systems.</i>	14
<i>Figure 2-4. The crystal structure of NiTi alloy (image reproduced from [3]).</i>	15
<i>Figure 2-5. Stress measurement of several actuators (image reproduced from [3]).</i>	16
<i>Figure 2-6. Strain measurement of several actuators (image reproduced from [3]).</i>	17
<i>Figure 2-7. Strain rate for the various actuators (image reproduced from [3]).</i>	18
<i>Figure 3-1. Norwood Abbey laser device.</i>	19
<i>Figure 4-1. Important values used in analysis of the device.</i>	21
<i>Figure 5-1. Prototype 1 components.</i>	27
<i>Figure 5-2. Device operation schematic</i>	28
<i>Figure 5-3. Nozzle solid model.</i>	29
<i>Figure 5-4. Orifice model.</i>	30
<i>Figure 5-5. Pressure-velocity curve for various orifice diameters.</i>	32
<i>Figure 5-6. Hamilton needle used as orifice.</i>	33
<i>Figure 5-7. Nozzle with 150 μm orifice.</i>	34
<i>Figure 5-8. Piston and cylinder solid model.</i>	35
<i>Figure 5-9. Wire pattern around the body.</i>	36
<i>Figure 5-10a,b. Design issues for the piston and cylinder components.</i>	37
<i>Figure 5-11. Completed piston and cylinder assembly.</i>	38
<i>Figure 5-12. Parallel and series wire configuration.</i>	39
<i>Figure 5-13. Capstan attached to the contacts.</i>	40
<i>Figure 5-14. Pulse power source (designed by Johann Burgert and Jan Malášek).</i>	41
<i>Figure 5-15. 25 V capacitor discharge through NiTi wire.</i>	42
<i>Figure 5-16. Injection test setup for Prototype 1.</i>	43
<i>Figure 5-17. Skin after injection from front and back.</i>	44
<i>Figure 5-18. Cross-section of skin after injection.</i>	44
<i>Figure 5-19. Discharge curve for 50 V capacitors.</i>	45
<i>Figure 6-1. Injection device module.</i>	49
<i>Figure 6-2. Measurements performed using Prototype 2.</i>	50
<i>Figure 6-3. Injection module.</i>	52
<i>Figure 6-4. Comparison of piston arrangement for Prototypes 1 and 2.</i>	53
<i>Figure 6-5. Solid model of pusher rod used in Prototype 2</i>	54
<i>Figure 6-6. Solid model of drug vial and piston</i>	55

<i>Figure 6-7. Drug vials for Prototype 2.</i>	56
<i>Figure 6-8. Ratchet tension system for Prototype 2.</i>	57
<i>Figure 6-9. Force gauge module used for skin contact force.</i>	58
<i>Figure 6-10. Position sensor module.</i>	59
<i>Figure 6-11. Calibration plot for the Omega linear potentiometer (the variance accounted for, R^2, by the fitted line also shown).</i>	60
<i>Figure 6-12. Typical recording from the position module.</i>	61
<i>Figure 6-13. Schematic of the break beam setup.</i>	62
<i>Figure 6-14. Break beam module.</i>	63
<i>Figure 6-15. Break beam module recording.</i>	64
<i>Figure 6-16. Pressure vessel used in pressure velocity experiments.</i>	65
<i>Figure 6-17. Pressure velocity experimental setup.</i>	66
<i>Figure 6-18. SolidWorks 2001 model of MK housing.</i>	67
<i>Figure 6-19. Test setup for injection test.</i>	69
<i>Figure 6-20. Typical injection test conducted with 2 mm drug vial.</i>	69
<i>Figure 6-21. Photo of pig skin before and after injection.</i>	70
<i>Figure 6-22. Experimental setup for drug velocity measurements.</i>	73
<i>Figure 6-23. Stream Velocity as a function of pressure.</i>	74
<i>Figure 6-24. Optimal piston diameter for Prototype 2 design.</i>	75

List of Tables

<i>Table 2-1. Needle-less injection products on the market.</i>	14
<i>Table 2-2. Table of NiTi properties.</i>	18
<i>Table 3-1. Overall device requirements</i>	20
<i>Table 5-1. Design criteria for Prototype 1</i>	26
<i>Table 5-2. Water properties at 20°C.</i>	30
<i>Table 5-3. Capacitors used in power supply.</i>	41
<i>Table 6-1. Design requirements for Prototype 2.</i>	51
<i>Table 6-2. Piston diameters used in the injection tests.</i>	68
<i>Table 6-3. Measurement results for injection test.</i>	71
<i>Table 6-4. Comparison of injection tests done with different capacitors.</i>	72
<i>Table 6-5. Comparison of the measured, theoretical and calculated velocities.</i>	73
<i>Table 6-6. Design parameters for drug vials from 3 mm to 5 mm.</i>	75

1 Introduction

This thesis explains the design and development of a needle-less injection device developed in the Bio-instrumentation laboratory at MIT. The needle-less injection device was designed to be hand-held, portable, reusable, and capable of accepting multiple types of drugs and drug volumes.

This thesis specifically focuses on Nickel-Titanium (NiTi) actuation methods for needle-less devices. NiTi wire contracts when heated and can be used as an actuation method for such devices. Heating was done by passing current through the wire, known as Joule heating. The current was supplied from a bank of capacitors and controlled using a pulse supply also constructed for this project.

A proof of concept device was created and is explained in detail in Section 5. It implemented some of the overall requirements and injected fluid into shoulder skin from a pig. The device has a 250 μL drug volume and has a drug speed measured at 90 m/s. The overall length was approximately 160 mm.

A second prototype was created to study the device operation and record values such as drug velocity, injection depth, skin contact force and energy requirements. This prototype was design as a test instrument as described in section 6 and was used to find optimal dimensions for many of the features. Drug vials were designed in varying diameters and tests were conducted on each.

It was found that an injection speed of 100 m/s or greater is necessary to penetrate the skin to a depth of 2 mm.

2 Background

2.1 Needle-less injection

Needle-less injection is the ability to transfer a drug from an injector through the skin without penetrating the skin with any part of the device. Most needle-less systems inject drug via a high speed stream. The drug passes through the skin into the desired layer, usually the fatty tissue. Figure 2-1 shows a schematic of injection via a typical needle-less system.

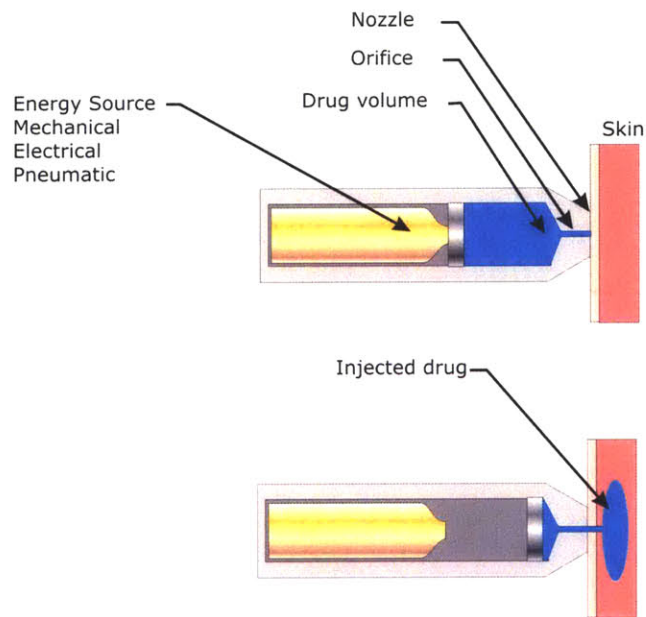


Figure 2-1. Injection method for needle-less injection systems.

In a needle-less injection system the fluid stream creates a local high pressure point at the skin's surface which punctures the skin allowing the drug to pass through. A stream diameter of approximately $100\ \mu\text{m}$ and traveling at $100\ \text{m/s}$ can achieve the desired injection depth of $2\ \text{mm}$ [18],[11]. A comparison of relative diameters for a 24 gauge (diameter of $460\ \mu\text{m}$) needle, a $100\ \mu\text{m}$ injection stream and a human hair is shown in Figure 2-2. From this figure it is seen that the needle-less stream is much smaller than the average injection needle.

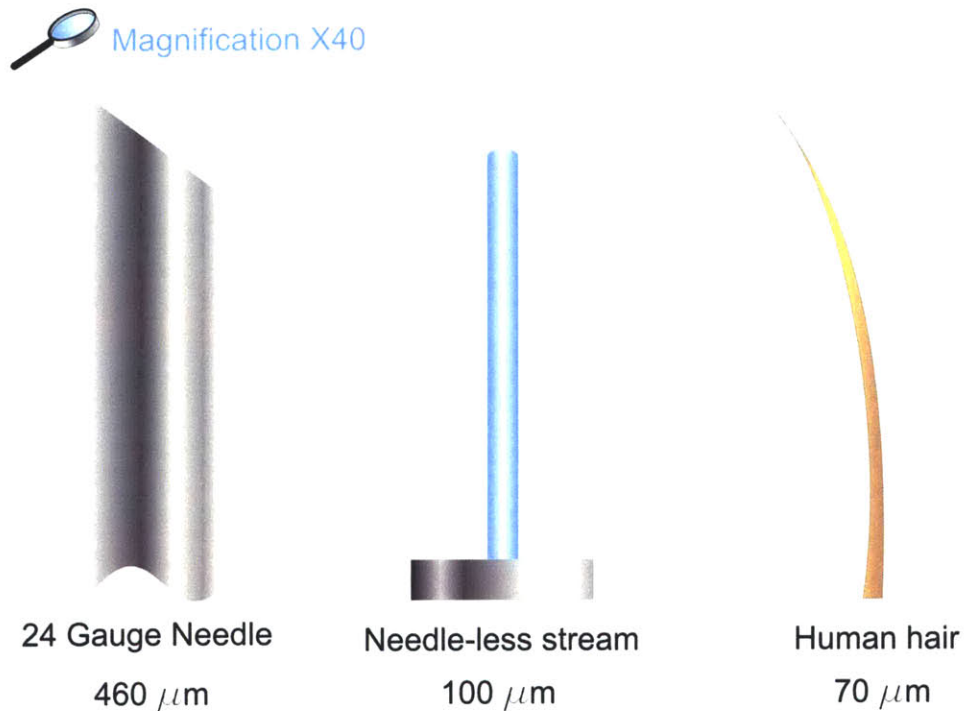


Figure 2-2. Size comparison of a human hair, 24 gauge needle and drug stream.

Needle-less injection has several advantages over conventional injection. Because there is no needle there is less chance of pricking or injecting the doctor or nurse. The injection device can be used quickly on different people with little threat of contamination. This increased safety and convenience makes the needle-less injection system a plausible replacement for many injections. This device could potentially be used in the home, doctor's office or in the field for large scale inoculations.

All needle-less injection systems developed to date have three components in common. The components essential to a needle-less injection system are a nozzle, drug reservoir and a pressure source. The drug volume holds the injection fluid inside the device. The nozzle provides the surface which comes in contact with the skin and the orifice which the drug passes through when injected. The energy source provides the necessary driving energy to the drug for injection. Figure 2-3 shows the basic layout of a needle-less injection device. The components of the needle-less injection device will be detailed in following sections.

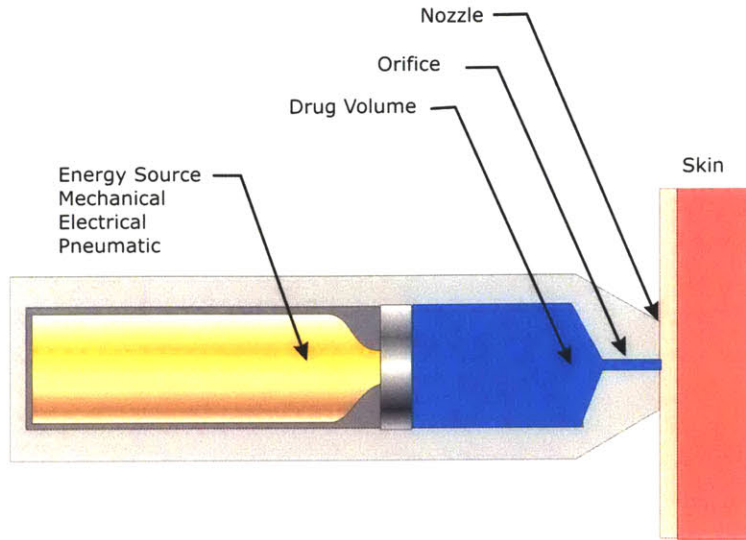


Figure 2-3. Basic components of most needle-less injection systems.

Many of the devices on the market use either mechanical or stored pressure as energy storage elements. The mechanical method stores energy in a spring which is released pushing a plunger to provide the necessary pressure. The pressure storage method uses compressed gas in a vessel which is released at the time of injection. Table 2-1 lists the main manufacturers of needle-less injection systems. Table 2-1 also lists the means of energy storage and other basic specifications for the various devices.

Table 2-1. Needle-less injection products on the market.

Needle-Less Injection Products							
Product	Company	Actuation Method	Depth of penetration	Drug Types	Drug Volume	Cycle Life	Source
Vision	Medijet	Spring	Subcutaneous	Insulin		3000	[11]
Injex	Injex	Spring	*	Insulin	.05 mL to 0.3 mL	*	[9]
Penjet	Penjet	Compressed Gas	*	Liquid	*	1	[13]
Intraject	Weston Medical	Compressed Gas	Subcutaneous	Liquid	0.1 mL to 0.5 mL	1	[18]
Powderject	Powderject	Compressed Gas	*	Powder Drug	*	*	[14]

* No data available

In this thesis shape memory actuation is used to create the necessary pressure for injection. The nickel titanium wire contracts when heated and thus produces driving force.

2.2 Shape memory alloy

Nickel titanium (Ni-Ti) alloy, also known as shape memory alloy (SMA) or Nitinol, is a shape memory material. NiTi has two stable phases, martensite and austenite. Martensitic transformations are at the heart of the shape memory effect [3]. A phase change occurs when the material is heated. The material has a different lattice structure in each state and the phase transformation causes a change in length.

Figure 2-4 shows the lattice structure of the two phases. In the austenite phase the crystal structure is body centered cubic. Although not fully understood, it is agreed that the crystal structure for the martensite phase is an orthorhombic crystal strained to a monoclinic crystal [3].

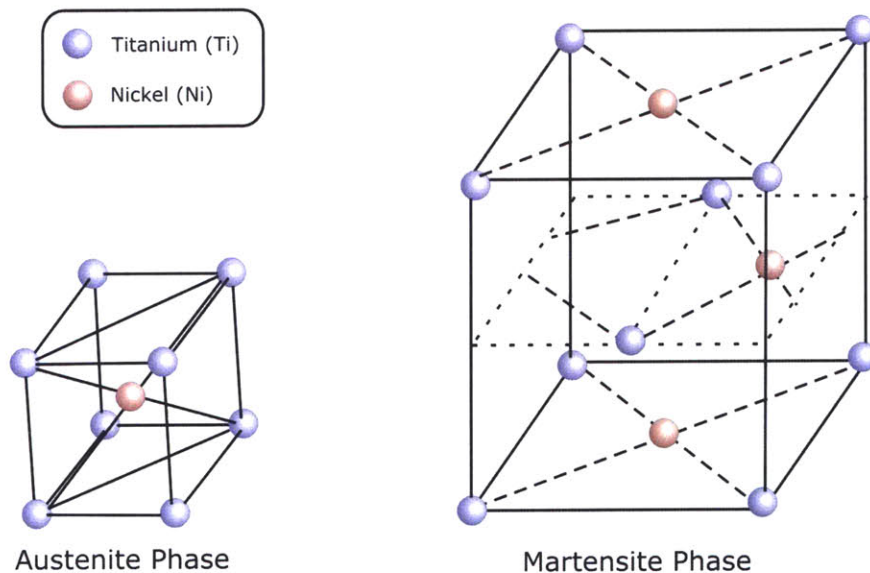


Figure 2-4. The crystal structure of NiTi alloy (image reproduced from [3]).

The shape memory effect was first observed by Arne Ölander in 1932 in gold-cadmium (Au-Cd) alloy [4]. Since then many alloys were discovered to have shape memory effect. There has been a particular focus on nickel-titanium (NiTi) alloy and much work has been done on applications for this alloy [3].

Nickel-titanium alloy is available in many forms such as wire, tube, ribbon and foil. The phase transition for nickel-titanium alloy typically ranges from 10 °C to 115 °C and depends on the exact makeup of the material. In general, the phase transition temperature increases as the nickel content is reduced [15].

Nickel-titanium alloy has very interesting and potentially useful mechanical properties. As an actuator, nickel-titanium alloy is remarkable. The stress that NiTi can generate is approximately 200 MPa and it can achieve strains of 5%. Stress and strain are shown in Figure 2-5 and Figure 2-6 along with other actuators.

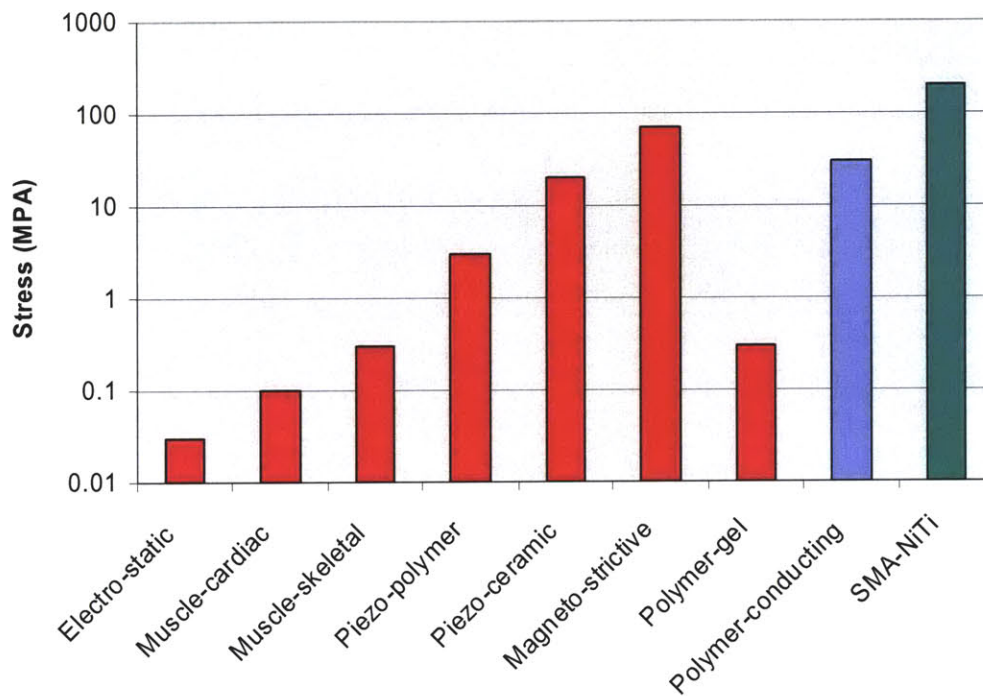


Figure 2-5. Stress measurement of several actuators (image reproduced from [3]).

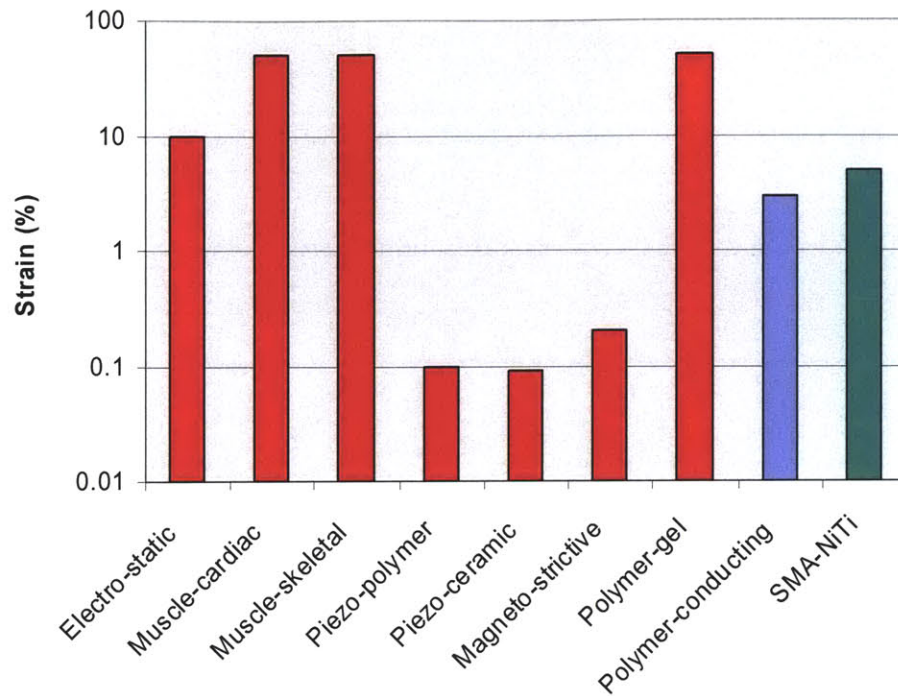


Figure 2-6. Strain measurement of several actuators (image reproduced from [3]).

Figure 2-7 shows the strain rates for the actuators in Figure 2-5 and Figure 2-6. The NiTi actuator has a large strain rate which results in extremely fast actuation. To reach the velocities required to inject through the skin the NiTi actuator shows the most promise of the actuation methods shown.

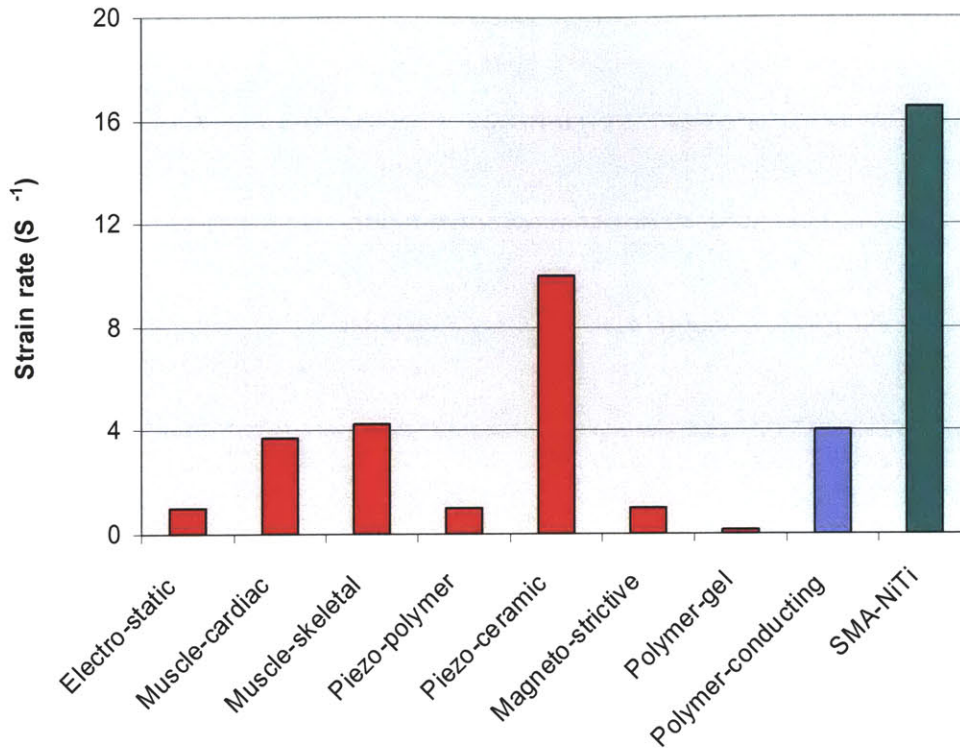


Figure 2-7. Strain rate for the various actuators (image reproduced from [3]).

The wire form of the nickel-titanium alloy was used for the needle-less injection system design and testing. The wire was purchased from Dyanlloy Inc [7], and has the following mechanical and electrical properties shown in Table 2-2 as measured in the lab:

Table 2-2. Table of NiTi properties.

Mechanical Properties			
Property	Value	Units	Test equipment
Diameter	0.371	mm	Laser scan micrometer
Activation Temperature	70	°C	Supplier Data
Strain	4.5	%	Ruler
Stress	200	MPa	Supplier Data
Electrical Properties			
Resistance	8.3	Ω/m	4 wire Ω meter

3 Overall Device Requirements

Design requirements were developed with consideration for existing medical devices. The device must contain three critical features: small size allowing device portability, low weight also for portability and the needle-less injection drug delivery. These three main features when examined yield a list of design requirements that will achieve the desired form.

Portability was a prime concern in the design requirements as the device is meant to be used in the field. The device was designed to be similar in size to the Norwood Abbey transdermal laser assisted delivery device which is used to remove the stratum corneum [12]. Figure 3-1 shows a solid model of the approximate shape and size of laser assisted delivery device.

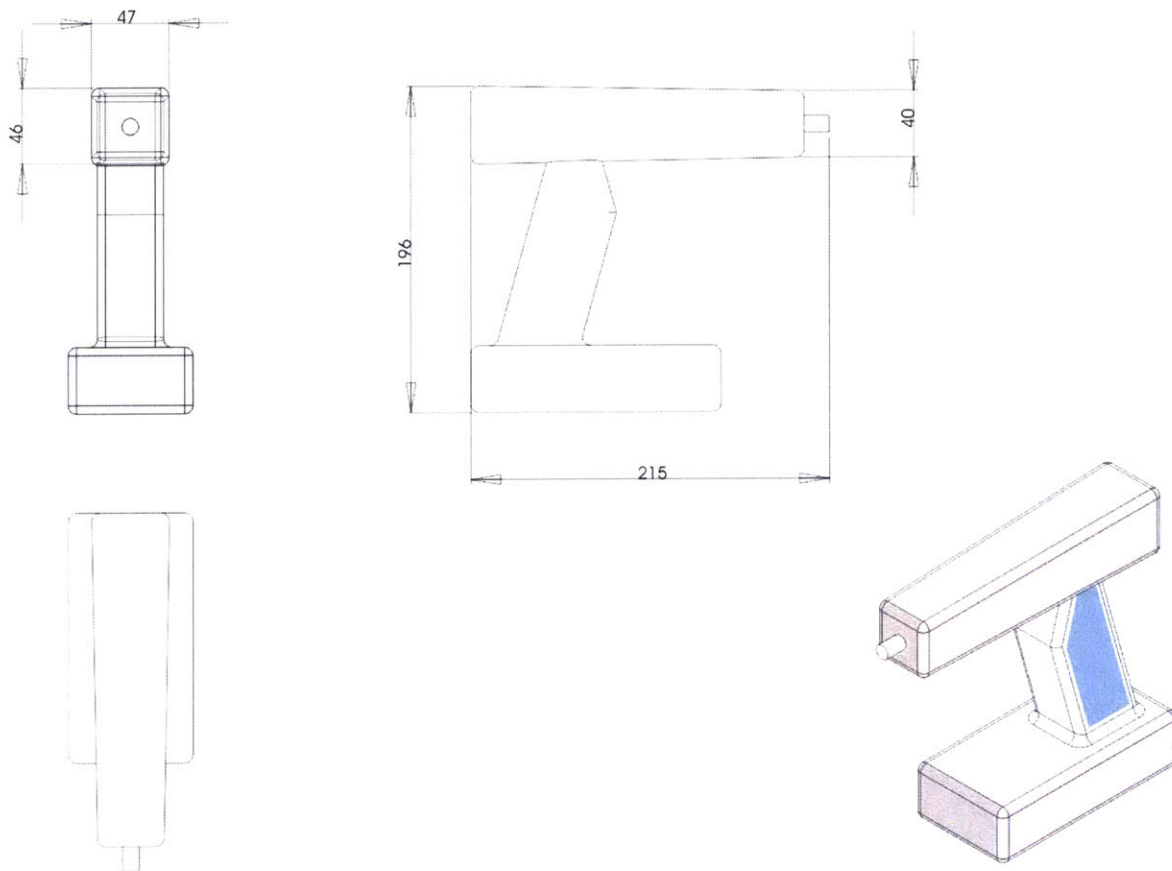


Figure 3-1. Norwood Abbey laser device.

The main barrel of the device has an overall length of 215 mm and a height and width of approximately 40 mm. The weight of the device is also a critical feature and should be

low enough that the device is easily carried. An acceptable weight for the device is approximately 1.5 kg. The device must not be tethered to a power source or other stored energy unit. The energy storage must be contained in the device.

A product feature which allows a single injector to inject several types of drugs or volumes of drugs would be beneficial. A disposable drug vial requirement was established to fulfill this need. These criteria define the product requirements which guide the development of the device and are listed in Table 3-1.

Table 3-1. Overall device requirements

Product Requirements
Hand held
Size < 215×40×40 mm
Weight < 1.5 kg
Portable
Stand alone device
Needle-less injection
Reusable injector
Disposable drug vial

4 Feasibility Analysis

The previous discussion described other devices on the market with actuation methods that differ from the proposed design using NiTi. Before any design work began, basic analysis of the governing equations was conducted to check the viability of using NiTi as an actuator. The feasibility analysis in this section shows that the design has promise and should be evaluated further.

The feasibility analysis focuses on four fundamental design and operation requirements. Any actuator used in a needle-less injection device must be capable of providing enough pressure to penetrate the skin. The drug must also be delivered at the specified fluid velocity. The energy consumption of the actuator during injections must be within the available energy specifications. Finally, the actuator and energy storage elements must be small enough to be handheld. Figure 4-1 contains all the necessary dimensions and material assumptions that are used in the analysis.

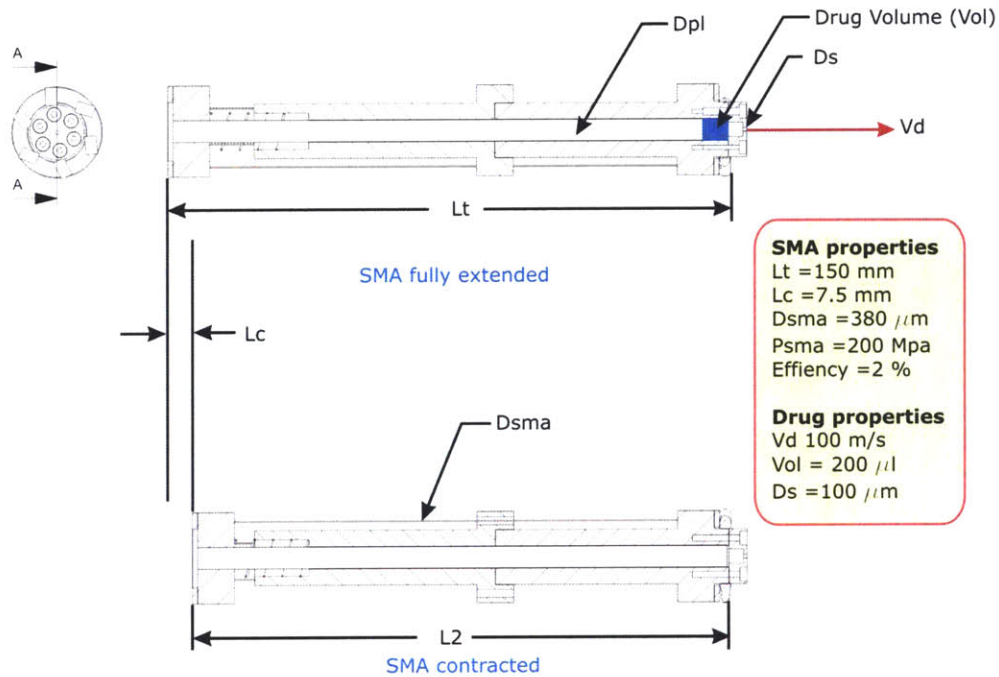


Figure 4-1. Important values used in analysis of the device.

4.1 Required pressure and fluid rate analysis

4.1.1 Pressure requirement

The pressure needed to penetrate the skin is generated using the NiTi actuator. The actuator applies force to a piston which causes a pressure increase on the drug volume. The drug contacts the skin at the orifice which is a small hole in the nozzle. The orifice in this analysis is 100 μm in diameter (D_s). Previous work showed that a needle of 100 μm diameter requires 0.15 N to penetrate the skin to a depth of 2 mm [1]. The approximate local pressure needed for an injection was obtained by dividing the force for the injection by the needle cross-sectional area and is found to be 1.91 MPa.

The volume of drug injected plays a critical role in the feasibility analysis. The NiTi actuation can generate a large force as shown in the properties of NiTi section. However the maximum strain in the material is only 5%. For the device to be hand held, the length of the device and thus the NiTi should be no longer than 150 mm. This leads to a contraction of 7.5 mm (L_c). Given this contraction length and a cylindrical drug

volume of 200 μL , a piston diameter of approximately 6 mm (D_{pl}) is needed to contain the required volume. This diameter results in a cross-sectional area of $8.48 \times 10^{-6} \text{ m}^2$ and is labeled P_{cc} in Figure 4-1. The force needed to generate the required pressure is the pressure multiplied by the piston area and is found to be approximately 162 N (F_{req}).

The NiTi actuator used in the feasibility analysis is 380 μm wire. Given a maximum stress of 200 MPa (see Table 2-2), the wire is capable of generating a force of approximately 23 N, thus the required force can be generated by placing approximately 7 NiTi wires in parallel. In this configuration the analysis shows that the NiTi actuator can generate the forces necessary to penetrate the skin.

4.1.2 Drug injection rate

It is generally accepted that a fluid velocity of 100 m/s is required for a successful injection [18],[11]. For NiTi to be a good candidate for the actuation of this device, it must be capable of expelling the fluid at the required velocity. This means the NiTi wire must be able to contract quickly thus creating the required fluid rate. Equation 1 shows the required strain rate ($\dot{\epsilon}$) as a function of drug velocity (V_d), piston area (A_{pl}), orifice cross-sectional (A_{cc}) area and total length of NiTi (L_t). The strain rate is found to be 0.185 s^{-1} which is less than the 16.5 s^{-1} NiTi is capable of producing.

$$\dot{\epsilon} = \frac{V_d \times A_{cc}}{A_{pl} \times L_t} \quad 1$$

4.2 Energy Requirements

The energy requirements for the NiTi actuator for a single shot can be approximated by simply calculating the work (W) done in expelling the drug and considering the efficiency of the NiTi. Equation 2 shows that, given a force required of 162 N and a contraction length of 7.5 mm, the theoretical energy requirement is 1.21 J.

$$W = F_{req} \times L_c \quad 2$$

This is an extremely small amount of energy, but we must take into account the efficiency of NiTi from electrical to mechanical energy which is less than 3% [3]. For the purposes of this analysis the efficiency of NiTi is assumed to be 2%. This gives a

total energy usage for one shot of 61 J. This energy can be supplied by the capacitors used in this experiment which provide 360 J/kg. At this energy density the weight of capacitors needed would be 0.166 kg.

4.3 Size requirements

The maximum size of the device was established in the background section and is shown in Figure 3-1. The proceeding analysis shows that the actuator as well as the energy storage element can fit required size constraints.

For a more detailed analysis refer to Appendix A, which contains a full analysis done in MathCAD [10].

5 Prototype 1 Design

5.1 Prototype design goals

To facilitate the design process for the needle-less injection device, a prototype was created. Prototype 1 is a proof of concept device. It verifies the feasibility analysis and shows that the NiTi is a viable actuator for a needle-less injection system. In addition to verification of the feasibility analysis Prototype 1 will also implement some of the design requirements that were stated in the background section. By implementing some of the design requirements in this first prototype, the design work needed in the final device will be reduced. Prototype 1 is, however, not designed for manufacture and is not considered a pre-market device. Many revisions are necessary before this product will be in final prototype stages.

5.2 Prototype 1 design considerations

In order to streamline and organize Prototype 1's design process, requirements for this particular prototype were established. These guidelines were developed from the design requirements and from the feasibility analysis. The requirements are meant to focus the design process and limit the prototype designs to ones that are useful to the overall goal. They also restrain the prototype so that it fits the theoretical model enough to be a verification of the analysis.

The requirements were developed from the feasibility analysis and the overall design requirements. The requirements focus on the structure, actuation and critical dimensions.

5.2.1 Structure

The device is required to be hand-held. Requirements were developed regarding the length and size of the device so that it would be small enough to meet the design requirement. The length of actuator was constrained to 150 mm which matches the length used in the feasibility analysis. The height and width measurements are constrained to less than 30 mm each. The main focus for this prototype is the actuation;

therefore, it was determined that the power source would not need to fall in these size requirements and did not have to be contained in the device.

Component modularity was designated a requirement, allowing easy design changes and more flexibility. Also, Prototype 1 had to undergo multiple tests and therefore had to be very robust.

5.2.2 Actuation

NiTi wire was chosen as the actuator for Prototype 1 due to its relatively low cost and availability. Joule heating is the most frequently used method of actuation for NiTi and is the method used in this prototype [3].

5.2.3 Critical dimensions

The critical dimension design requirements were obtained from the feasibility analysis. The required injected drug volume was 200 μm , with a drug speed of 100 m/s.

5.2.4 Criteria

The design criteria described in Sections 5.2.1 through 5.2.3 are summarized in Table 5-1 below.

Table 5-1. Design criteria for Prototype 1

Criteria	Description
Size	Hand Held
Length	150 mm
Height width	30×30 mm
Overall design	Modular
Life	Multiple Use
Construction	Robust
Actuation	NiTi wire
Actuation method	Joule Heating
Drug Volume	200 μ m
Injection Speed	100 m/s
Injection pressure	1.91 MPa

5.3 Prototype Design

5.3.1 Overall device

Prototype 1 was designed as a modular system with several independent parts, which combine to create the overall device. The main components of the system are shown in Figure 5-1 and are as follows: the nozzle, piston, cylinder, NiTi actuator, electrical contacts and power source. The design of each of these components will be discussed in the following sections.

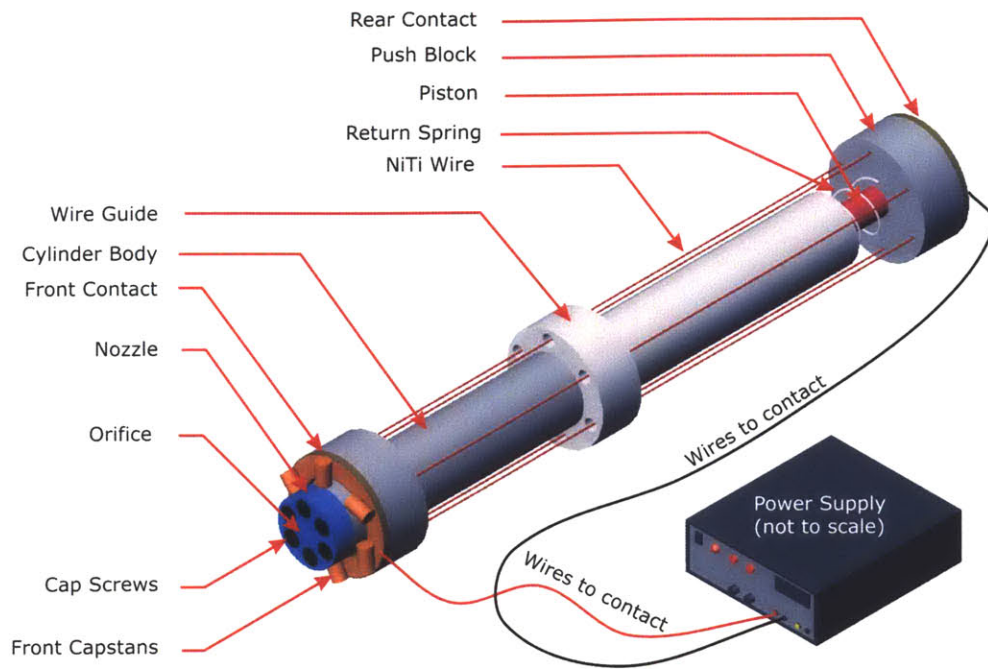


Figure 5-1. Prototype 1 components.

Prototype 1 operates by applying pressure to the liquid in the drug chamber by means of a piston and cylinder. This pressure drives the fluid through the drug nozzle into the skin. The pressure is achieved using NiTi wires around the piston cylinder apparatus. Figure 5-2 shows the basic concept employed in this design.

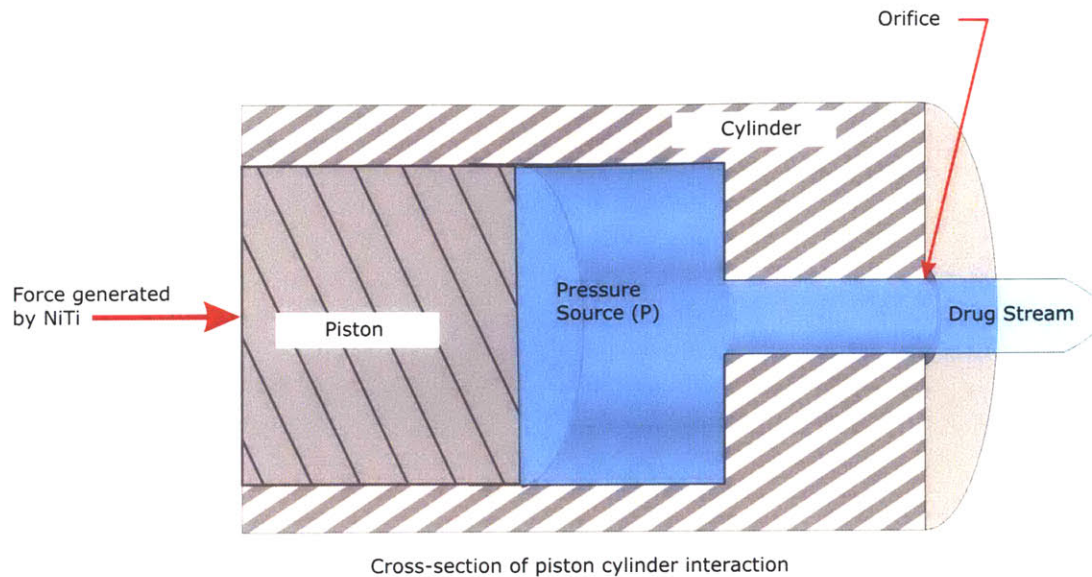


Figure 5-2. Device operation schematic

5.3.2 Nozzle

The nozzle has two critical functions: it acts as the passage for the drug and as the surface which contacts the skin. The nozzle contains a flat surface and an orifice. In this prototype, the nozzle is a cylinder which has an orifice in the center. Figure 5-3 shows the solid model of the nozzle.

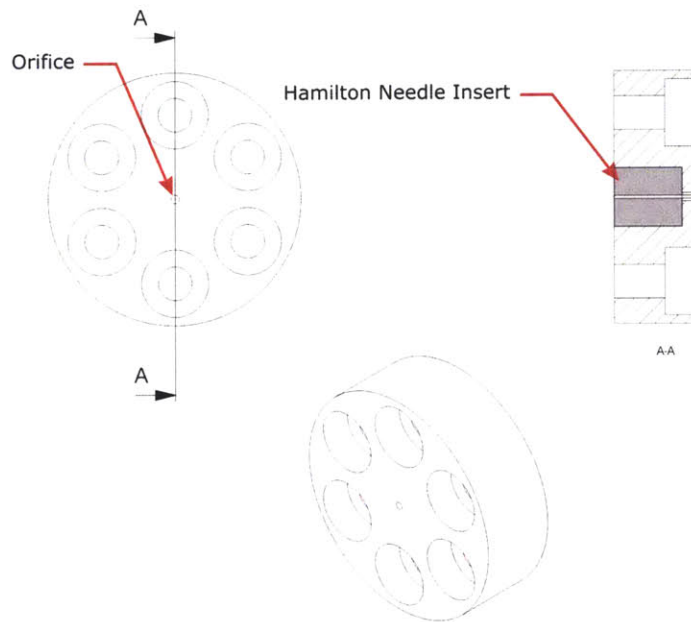


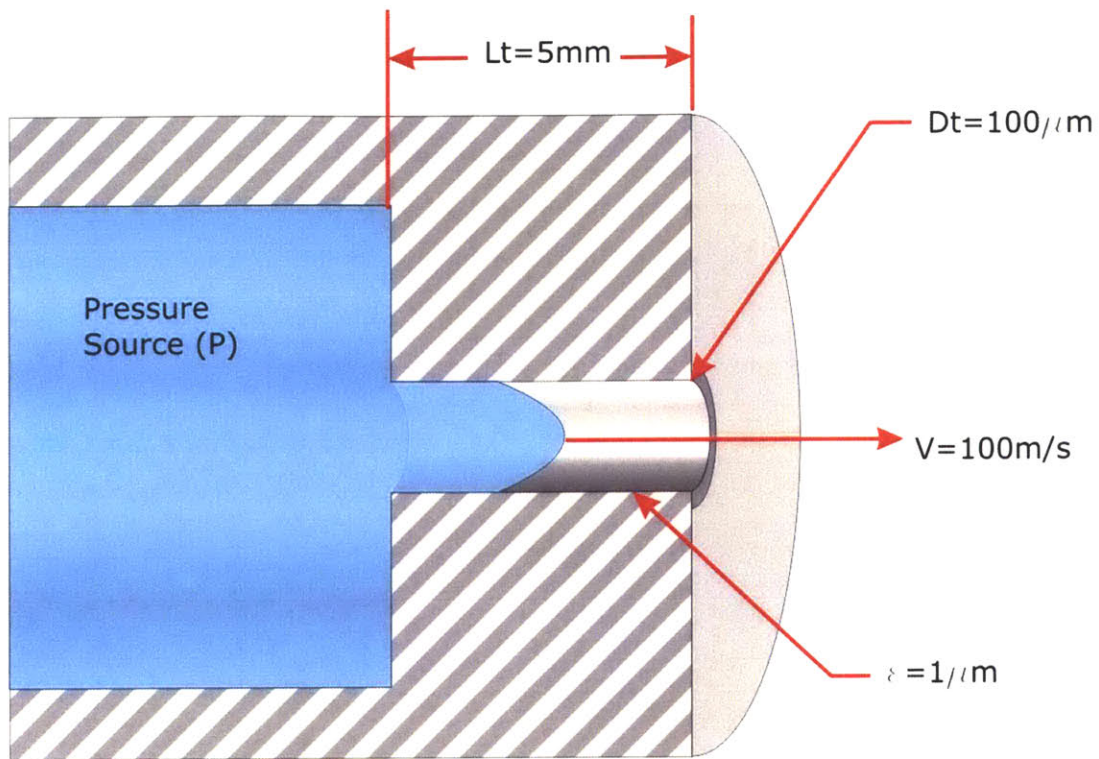
Figure 5-3. Nozzle solid model.

This nozzle is attached via screws to the cylinder containing the drug thus sealing the drug volume. The nozzle was designed to convey the drug to the skin at the required speed and diameter to penetrate the skin as determined in the feasibility analysis.

5.3.2.1 Orifice

The orifice controls the drug stream diameter and speed. The speed of the fluid depends on the diameter and the NiTi contraction time. The diameter of the orifice controls the diameter of the drug stream. The orifice must be designed so that the NiTi can provide the necessary pressure to drive the fluid. For this reason the pressure drop through the orifice must be considered. A model of the orifice was created using standard fluid dynamics to solve for the pressure required.

The orifice was modeled as a tube of length (L_t) and diameter (D_t). The tube is in contact with a pressure source from which the fluid flows. Fluid flows from the pressure source through the tube at velocity (V) Figure 5-4 shows a sketch of this system.



Nozzle Cross-section

Figure 5-4. Orifice model.

Due to the availability of tubing used to create the orifice, the diameter (D_t) in this analysis was changed to $150 \mu\text{m}$ from $100 \mu\text{m}$ used in design requirements. This change to the orifice diameter lowers the number of wires needed to inject the fluid to approximately 4.

For the purpose of analysis and testing, it is important to note that colored water was used as the test drug. This will be important as many values for the equations rely on the drug material properties. Table 5-2 shows the approximate material properties of water at room temperature.

Table 5-2. Water properties at 20°C.

density ρ	viscosity μ
998 kg/m^3	$1 \text{ mN}\cdot\text{s/m}^2$

A Reynolds number of 14970 was found using Equation 3 assuming water properties in Table 5-2 a 100 μm orifice diameter and 100 m/s drug velocity. Flows with a Reynolds number above 2300 are considered turbulent [6].

$$\text{Re} = \frac{\rho \cdot D_t \cdot V}{\mu} \quad 3$$

The driving pressure required for a fluid velocity of 100 m/s through the 150 μm diameter orifice as a function of tube length was found using the 4 from which gives the pressure drop for turbulent flow. The tube surface roughness (ϵ) was set to 1 μm . The tube length was varied until the pressure was larger than the pressure determined in the feasibility analysis (1.91 MPa). Given this pressure the maximum tube length was found to be less than 12 mm. A tube length of 5 mm was chosen for the design.

$$f = \left[\frac{1}{-1.8 \cdot \log \left[\left(\frac{6.9}{\text{Re}} \right) + \left(\frac{\epsilon}{\text{Dt}} \right)^{1.11} \right]} \right]^2, \quad 4a$$

$$\text{hf} = f \cdot \frac{\text{Lt} \cdot V^2}{\text{Dt} \cdot 2g}, \quad 4b$$

$$\Delta P = \rho \cdot g \cdot \text{hf} \quad 4c$$

Substituting 4b into 4c we get 4d (pressure drop as a function of tube length Lt)

$$\Delta P = \frac{(\rho \cdot f \cdot V^2) \cdot \text{Lt}}{2\text{Dt}} \quad 4d$$

Figure 5-5 shows the pressure-velocity relationship for orifice diameters ranging from 50 μm to 200 μm .

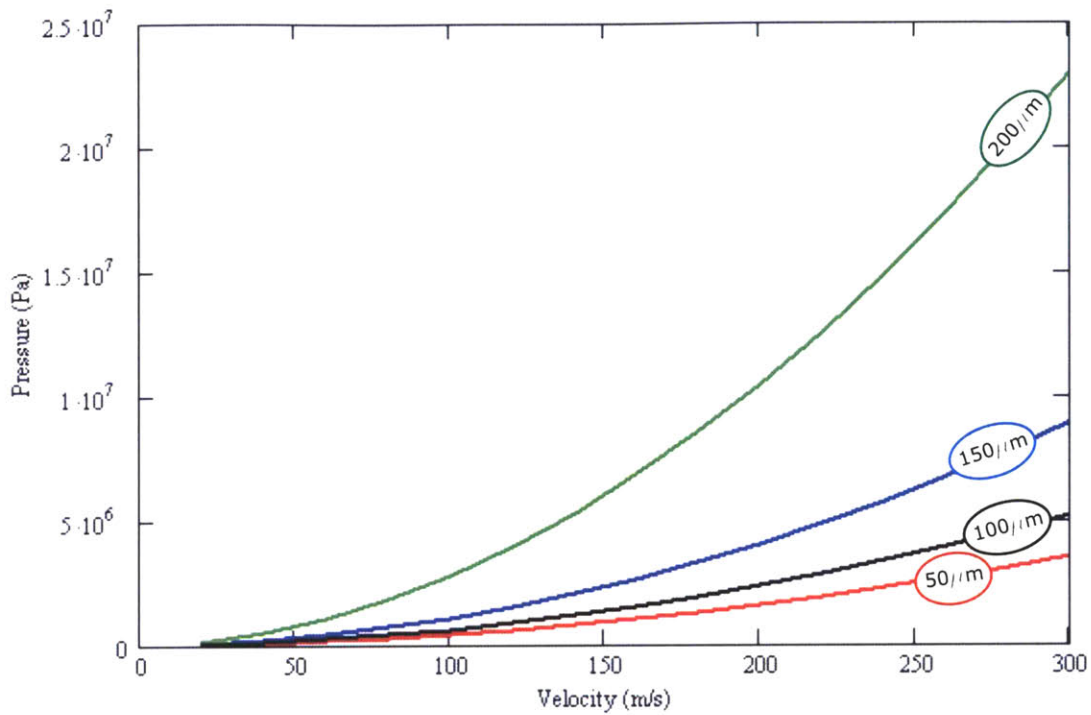


Figure 5-5. Pressure-velocity curve for various orifice diameters.

A detailed analysis can be found in Appendix B.

5.3.2.2 Machining and Assembly

The nozzle is constructed from aluminum for its ease of machining and strength. Six 2.5mm cap screws are used to secure the nozzle to the cylinder. This ensures that there will be no leakage between the cylinder and the nozzle.

The orifice was created using a stainless steel injection needle with a diameter of 150 μm (Hamilton needle part number 79631) shown in Figure 5-6.

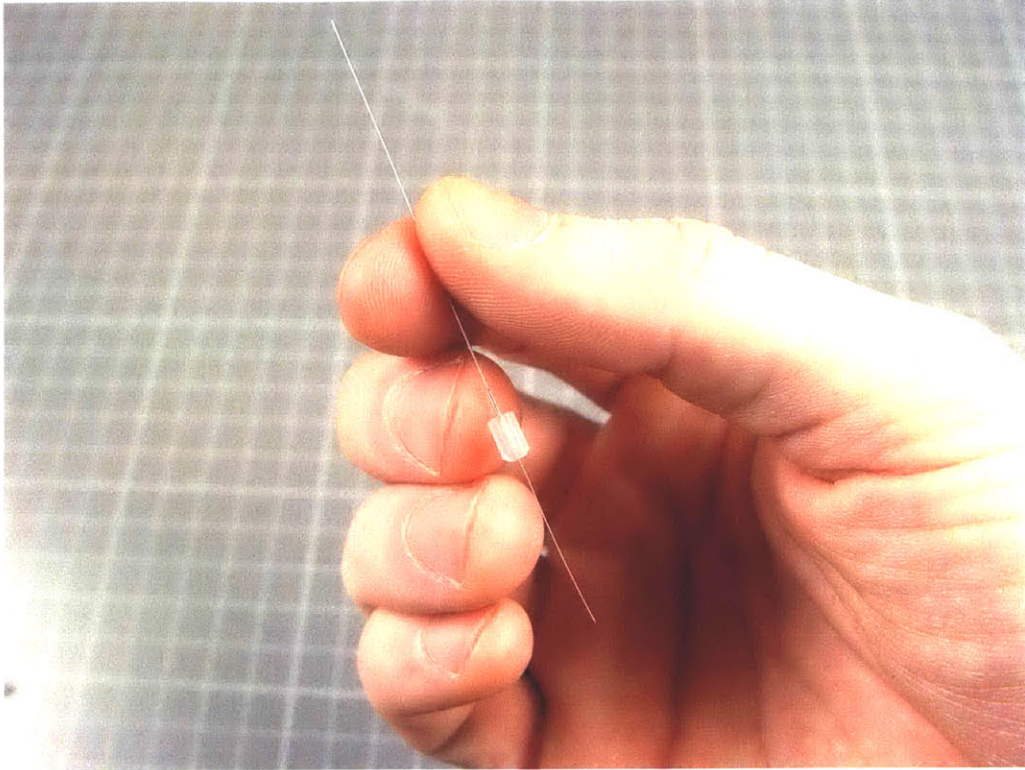


Figure 5-6. Hamilton needle used as orifice.

The Hamilton needle was chosen for its many size ranges and availability. The needle was attached to the nozzle using Hardman 5-minute epoxy. After the needle was fixed in place, the ends were cut and ground for a flat surface. The final nozzle used on Prototype 1 is shown in Figure 5-7.

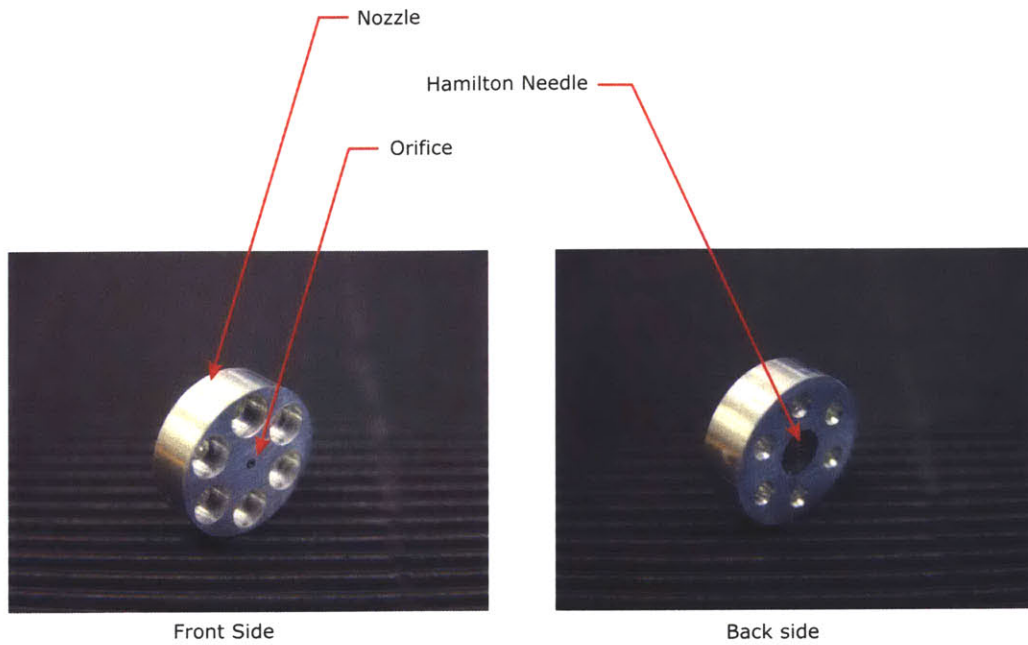


Figure 5-7. Nozzle with 150 μm orifice.

5.3.3 Piston Cylinder

The piston and cylinder, combined with the nozzle, form the drug volume as well as the body of the device. Attaching the nozzle to the end of the cylinder as stated in the previous section closes a drug volume. As the piston contracts the drug is expelled through the orifice. The solid model of the piston and cylinder is shown in Figure 5-8.

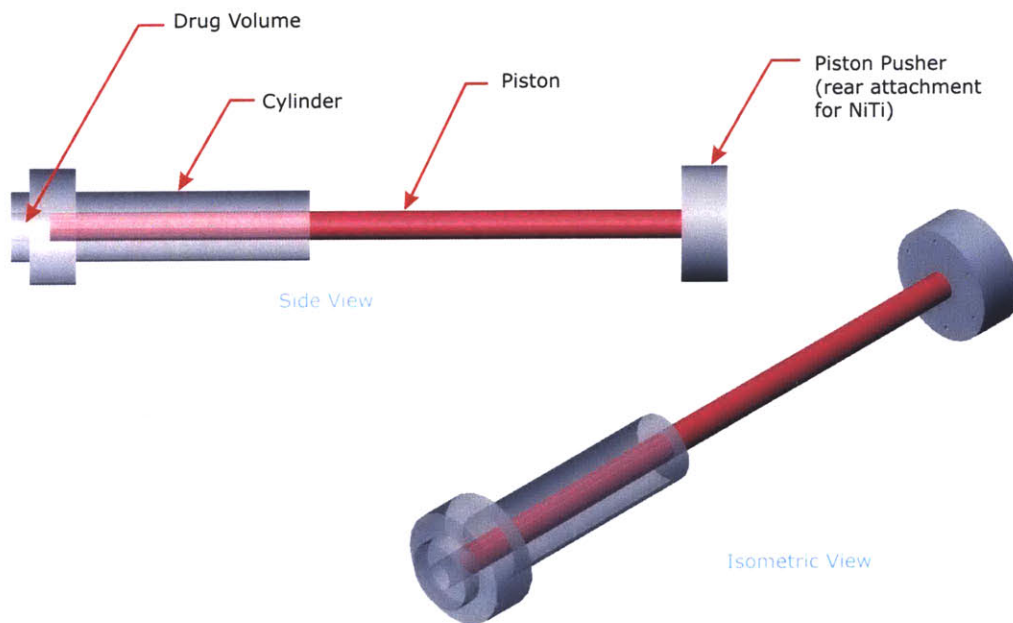


Figure 5-8. Piston and cylinder solid model.

From the feasibility analysis the drug volume and piston diameter were determined to be 200 μL and 6mm respectively. The length of the cylinder body was made 70 mm to prevent binding from the piston rod. The piston rod was made sufficiently long to accommodate the length of NiTi wire. From the feasibility analysis the length of the NiTi wire was calculated to be 150 mm for a 7.5 mm contraction. The NiTi is attached in a cylindrical pattern around the body as shown in Figure 5-9. The NiTi is attached to the cylinder close to the nozzle. In order to fit the proper length of NiTi, the piston rod had to be approximately 160 mm

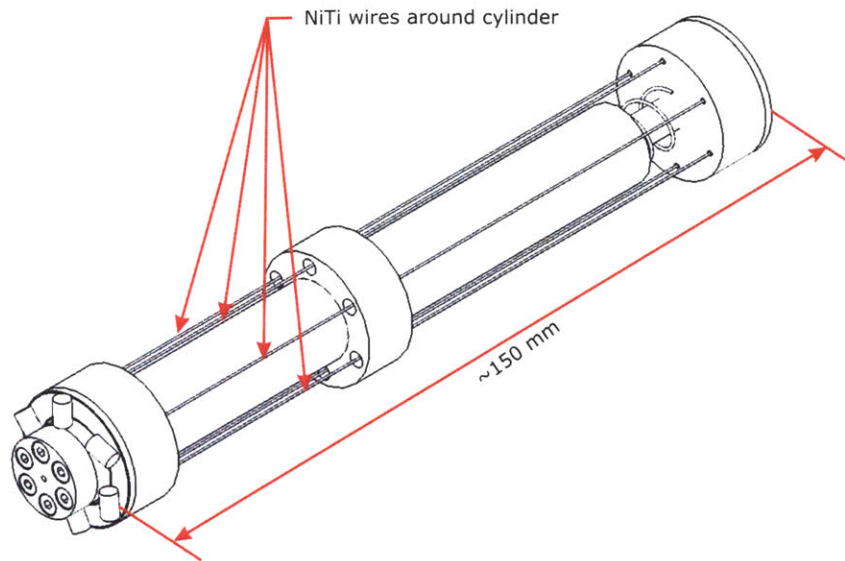


Figure 5-9. Wire pattern around the body.

There are several issues that arise from the high pressure contained in the chamber. The piston and cylinder as stated before hold the drug and force it out during the injection. Therefore the pressure needed to force the drug out the nozzle will be exerted in all directions inside the chamber. The high pressure may cause a rupture in the cylinder wall if it is too thin. If the piston is not sufficiently sealed with the cylinder there may be leakage around the piston. Both of these issues are shown in Figure 5-10

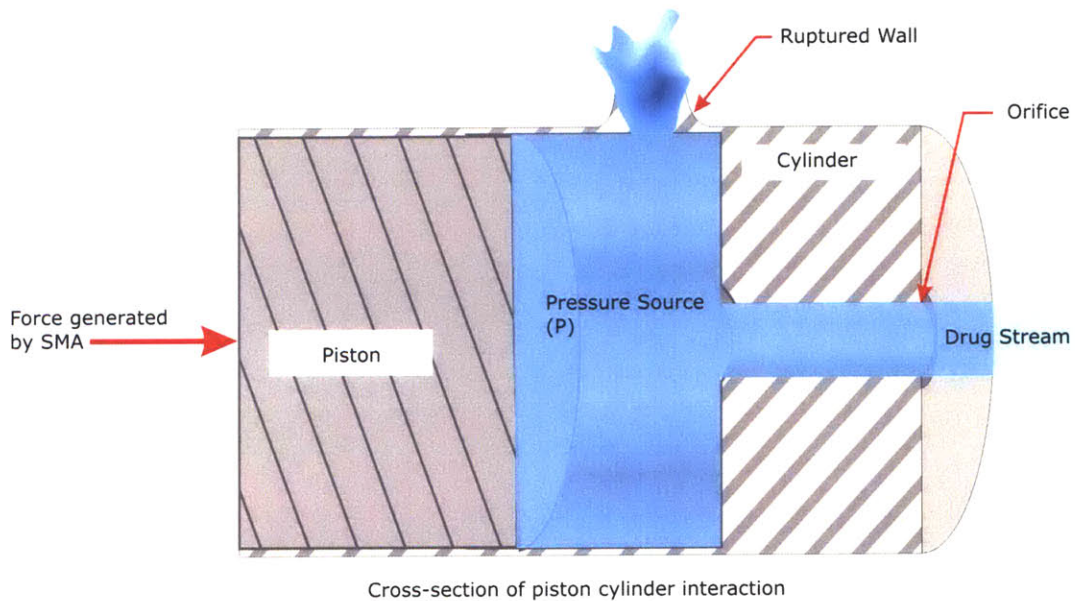
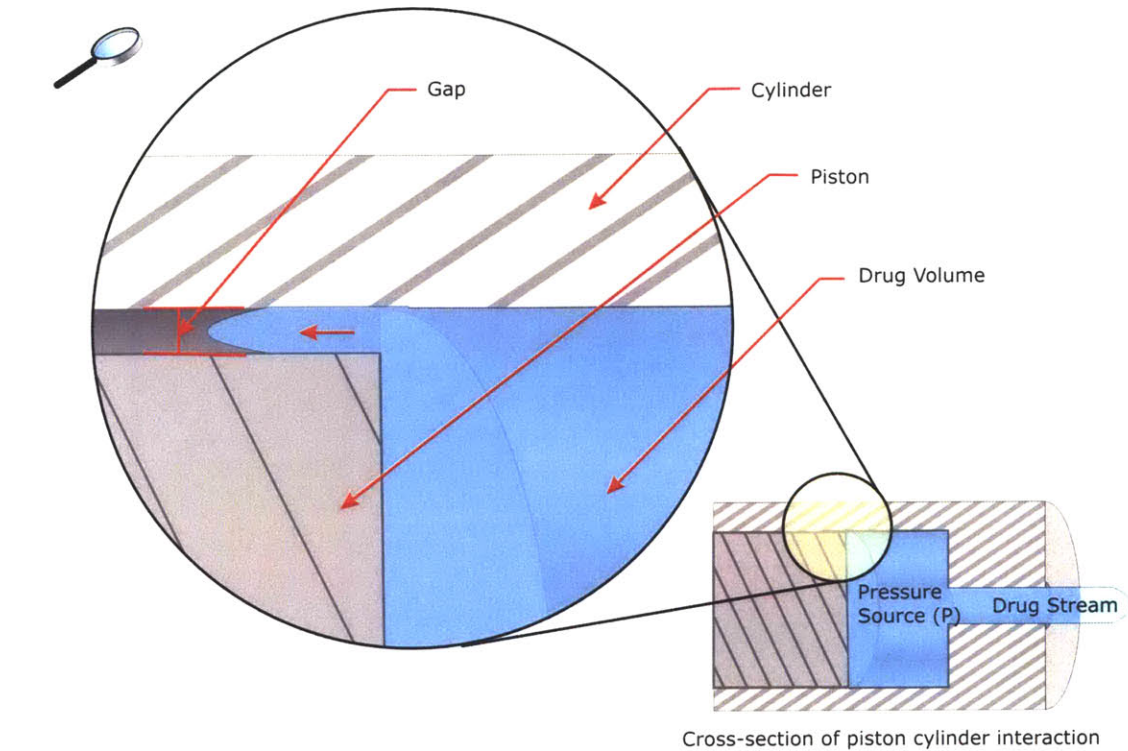


Figure 5-10a,b. Design issues for the piston and cylinder components.

To find the appropriate thickness, the hoop strength of the cylinder was checked. This stress should be less than the yield stress of the cylinder material to prevent rupture. This equation can be seen in Appendix C. The cylinder was made of aluminum which has

minimum yield strength of 35 MPa [2]. The equation shows that a wall thickness of 2 mm is required. A wall thickness of 4.5 mm was chosen for the design to include a factor of safety.

To design for leakage, the pressure drop must be considered. To simplify the calculation, the piston and cylinder were modeled as two parallel plates separated by a gap. Assuming a 50 μm clearance, calculations (see Appendix C) show that the pressure drop across the piston cylinder interaction is far greater than the pressure drop through nozzle if the length of the interaction is 60 mm. This insures that the piston cylinder will not leak during injection.

5.3.3.1 Manufacture and assembly

The piston cylinder was constructed using round aluminum stock and turning it to the proper dimensions. A diameter of 25 mm was made on the end for mounting. Holes were drilled around the diameter for the NiTi actuator. The center hole which becomes the drug volume was reamed to 6 mm. A precision stainless steel rod was used as the piston. This rod was chosen for its availability and precision dimensions. Figure 5-11 shows the piston and cylinder components

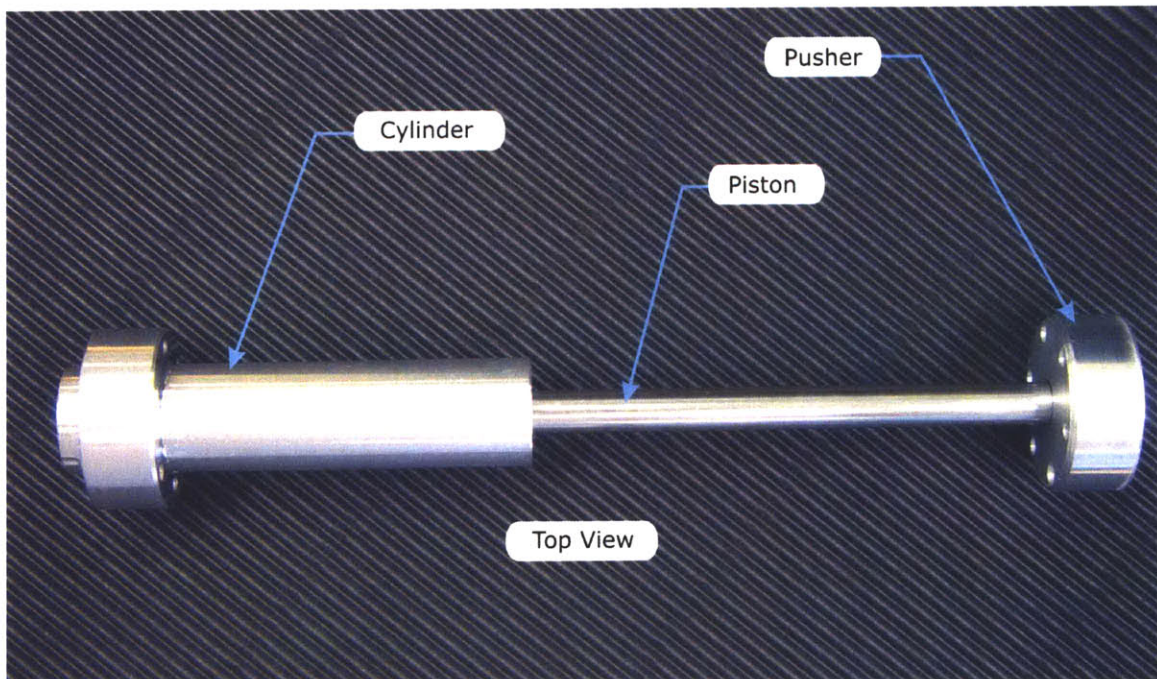


Figure 5-11. Completed piston and cylinder assembly.

5.3.4 NiTi actuator

Actuation of the device was accomplished using 6 wires in evenly spaced intervals around the device. The wire used for actuation was 380 μm NiTi wire with a 70 °C activation temperature. Material properties are listed in Table 2-1. The feasibility analysis shows that 7 wires are required to generate pressure however the change in orifice diameter from 100 μm to 150 μm results in a need for 4 NiTi wires. Six wires were used in the design of the device as a factor of safety. The predicted force generated by the six NiTi wires is 136 N.

5.3.4.1 Wire diagram

The two main wiring schemes are parallel and series connections. Each is shown in Figure 5-12 below.

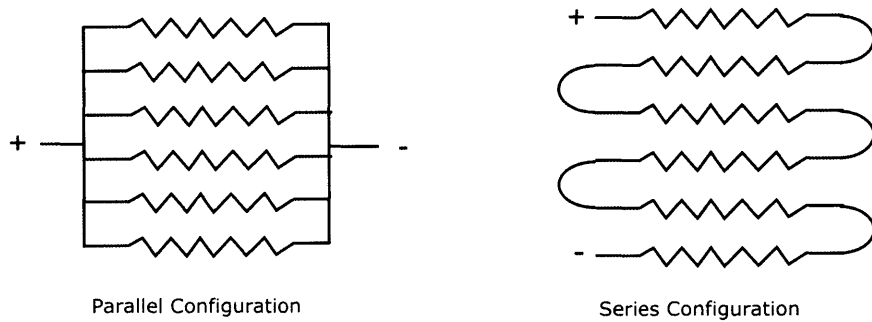


Figure 5-12. Parallel and series wire configuration.

The parallel configuration shown in Figure 5-12 was chosen due to its lower resistance. The theoretical resistance is found using Equation 5, using the wire resistance of 8.3 Ω/m (ρ), number of wires ($N=6$) and the wire length ($L=150$ mm). The system resistance is thus 0.208 Ω (R_t).

$$R_t = \frac{\rho m \cdot L}{N} \quad 5$$

5.3.4.2 Contacts

The contacts provide a connection for the power source and send the current to the NiTi actuator. In the parallel wire configuration, the contacts are arranged to connect one end of all the wires together with one contact and the other to a second contact.

The wires are attached to the contacts using capstans shown in Figure 5-13. Due to the forces generated by the NiTi wire during actuation, conventional clamps would not hold.

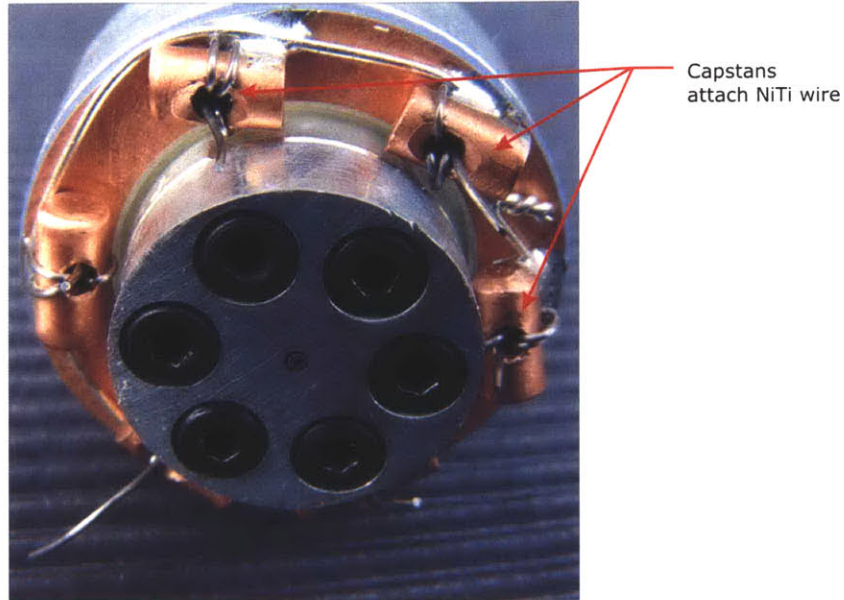


Figure 5-13. Capstan attached to the contacts.

5.3.5 Power Source

As stated earlier, the wires contract when heated. The method for heating the wires is joule heating. In order to achieve the required contraction times, the wire must be heated quickly, thus large currents of approximately 25 to 100 A are required.

Capacitors were used to supply the necessary energy pulse. Capacitors have the capability to supply large power density on the order of 7000 W/kg. They, however, do not have large energy densities so they must be charged by batteries for every shot. Batteries have the necessary energy densities needed to charge the capacitors, approximately 360 J/kg. To control the pulse, a power source was constructed. The power source has the ability to switch the large currents and voltages with millisecond timing. The power source also charges the capacitors to their required charge. Figure 5-14 shows the charging device and labels the interface.

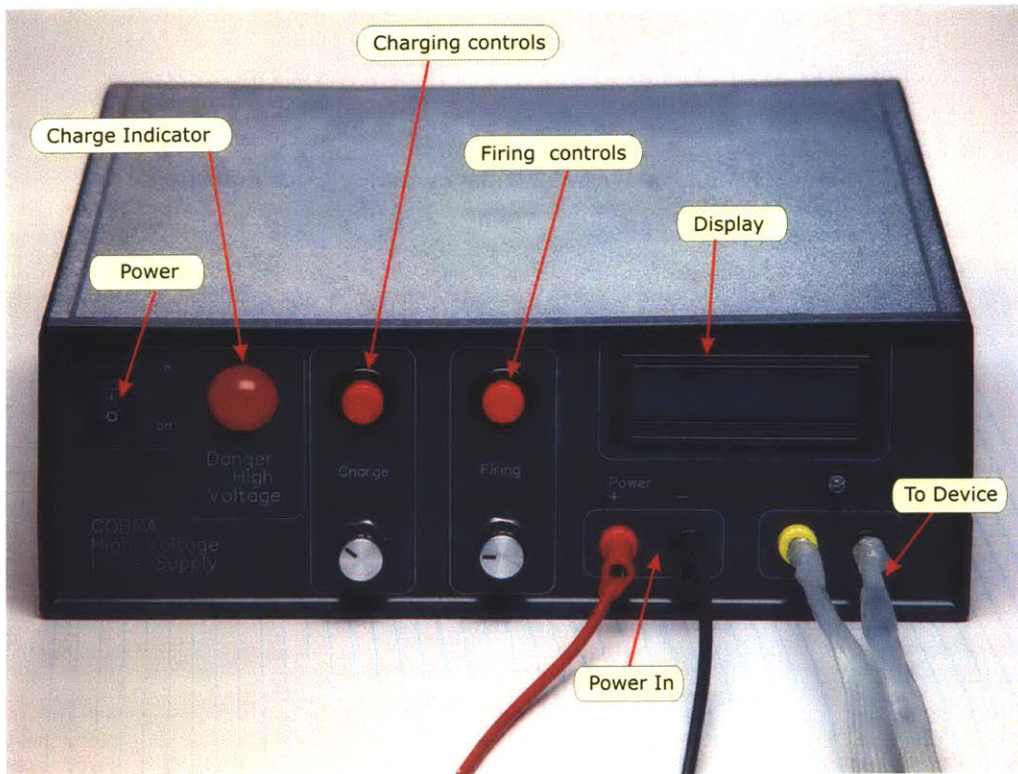


Figure 5-14. Pulse power source (designed by Johann Burgert and Jan Malášek).

The device operates by charging the capacitors using an inductor to increase the voltage to the required level. The power source has the ability to charge up to 100 V. When the capacitor bank is charged a switch is used to fire the pulse. FET switches controlled by the micro-controller control the pulse length capacitor bank. Appendix D shows the power supply circuit.

The capacitors used are listed in Table 5-3. The energy dissipated during a single 50ms pulse is calculated using the measured resistance of the device 0.7Ω .

Table 5-3. Capacitors used in power supply.

Voltage (V)	Capacitance (F)	Total energy* (J)	Energy dissipated in 50 ms** (J)
25	0.400	125	38
50	0.156	195	116
100	0.048	240	227

* based on $1/2 CV^2$

** Based on resistance of 0.7Ω

It can also be seen that the required energy for a given volume as calculated in the feasibility analysis is lower than the energy contained in 50 V and 100 V the capacitors.

A test of the capacitor discharge for the power sources was performed and the results are shown in Figure 5-15.

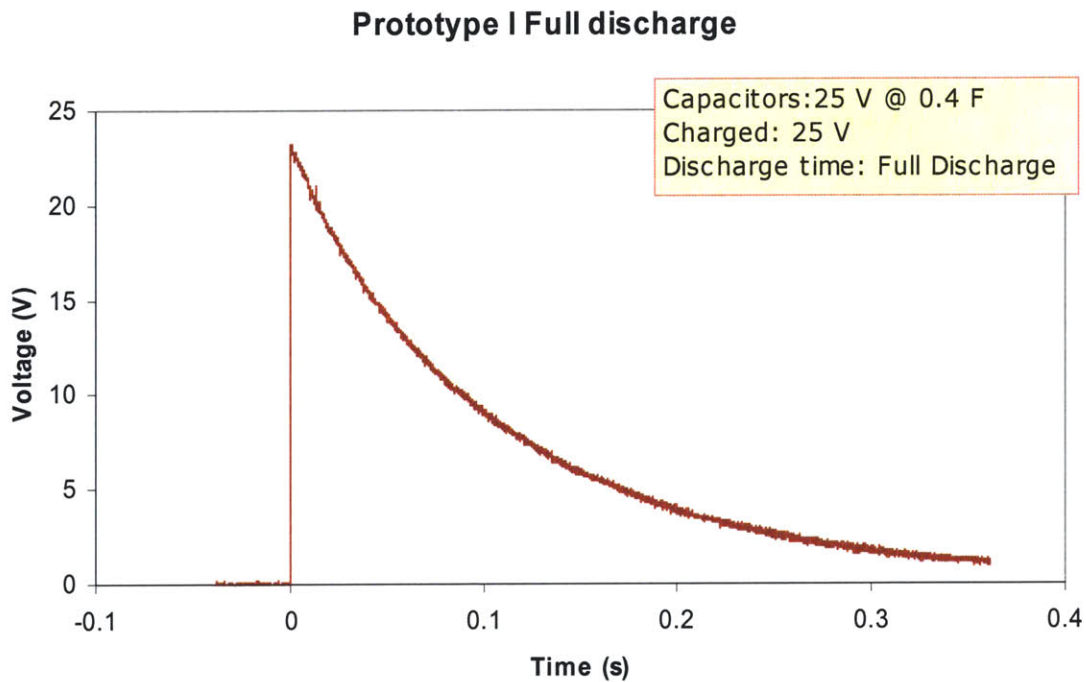


Figure 5-15. 25 V capacitor discharge through NiTi wire.

5.4 Prototype 1 Testing and Analysis

Injection and power usage tests were performed as a proof of concept for the device. The injection test was subjective and was analyzed by examining the skin once an injection was complete. The energy consumption was tested by measuring the voltage supplied to the device while firing.

5.4.1 Injection Test

The injection test was done by placing a square patch of pig skin against the nozzle and injecting Coomassie Blue a protein dye. The pig skin was cut from the shoulder of a pig. This tissue has structure and dimensions resembling that of human skin [5]. The setup is shown in Figure 5-16 labeling various parts of the setup.

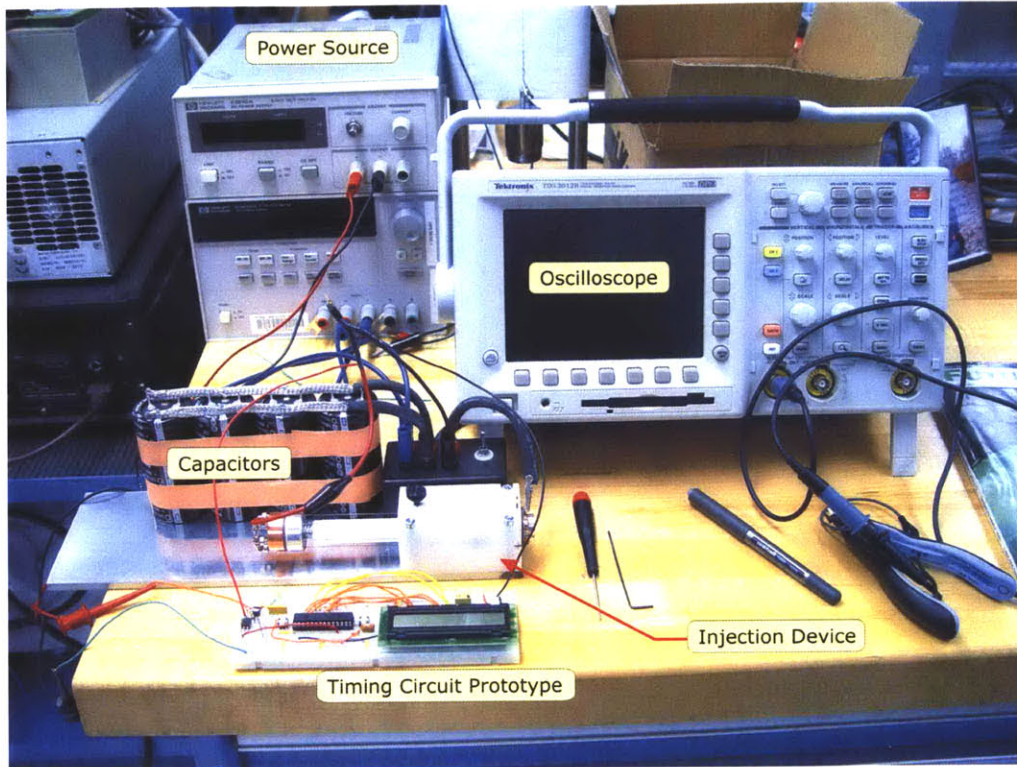


Figure 5-16. Injection test setup for Prototype 1.

During the test, the pig skin was pressed against the nozzle by an applied force. The device was then activated using the power supply. Once the injection was complete, the skin was removed and examined. The skin was first examined from the front then the back for dye penetration. Figure 5-17 shows a skin trial after injection from the front

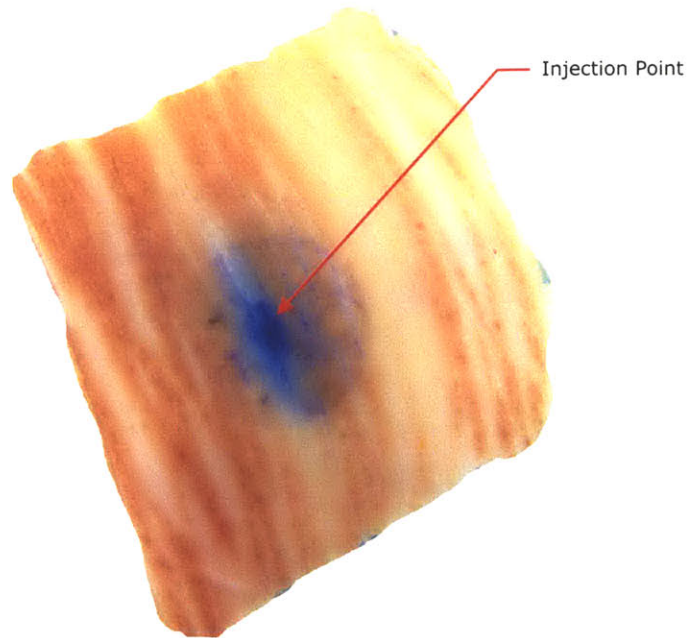


Figure 5-17. Skin after injection from front and back.

Once the outer part of the skin was examined the skin was cut with a scalpel to determine the depth of penetration. Figure 5-18 shows the skin from the side. It can be seen in the figure that the penetration is through the outer layer of skin

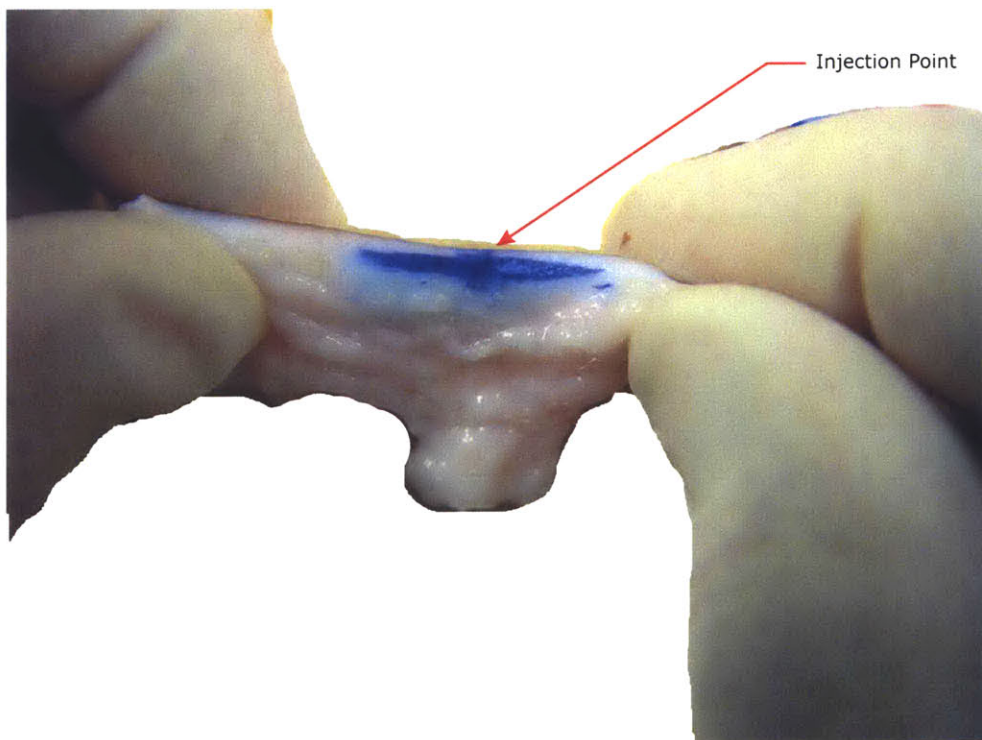


Figure 5-18. Cross-section of skin after injection.

The injection was tested on several pieces of skin and at several voltages. See the Appendix E for other pictures of injection tests.

5.4.2 Discharge test

A Tektronix 2014 digital oscilloscope was attached to the contacts of Prototype 1 during the injection test to measure the voltage as a function of time. By measuring the voltage over the discharge period and the resistance for the NiTi wire system, approximate energy consumption can be found. This was done by fitting a curve to the voltage data $V(t)$ and integrating the result using,

$$P = \int_{t_0}^{t_1} \frac{V(t)^2}{R} dt . \quad 6$$

A typical discharge curve looks like Figure 5-19, which has all the relevant data on it. Using an exponential function to fit the voltage data the approximate power dissipated was 57J.

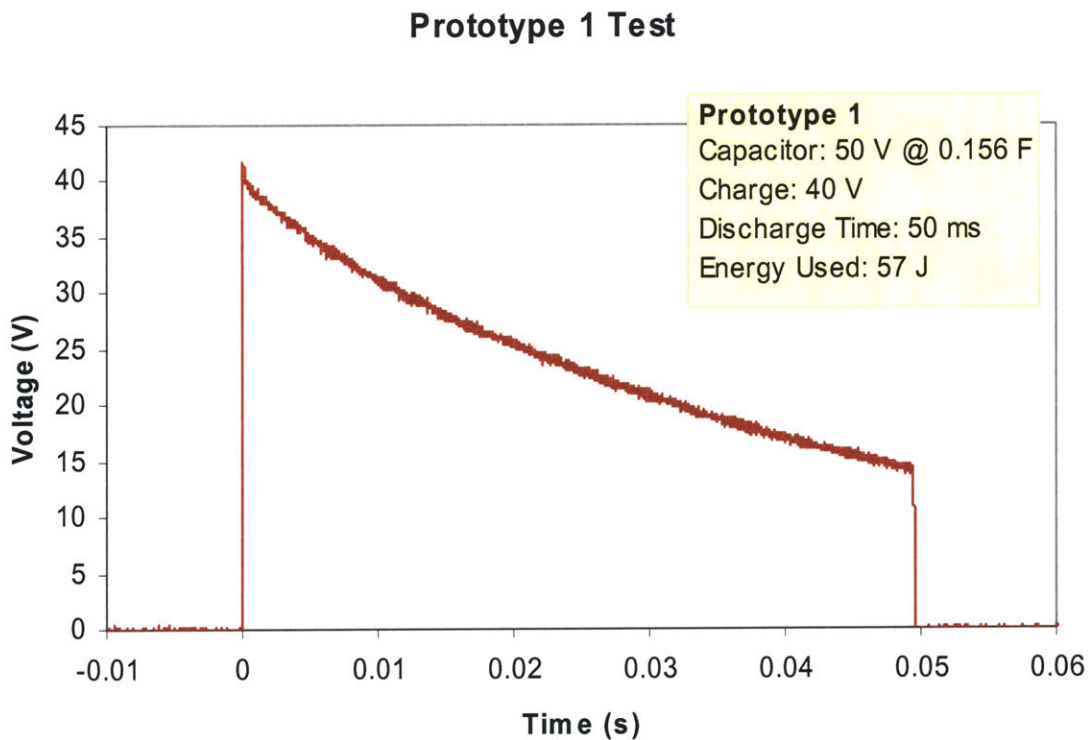


Figure 5-19. Discharge curve for 50 V capacitors.

5.5 Prototype 1 Design analysis

Prototype 1 was designed to test the basic design and some of the overall design requirements. It demonstrates that the idea is a viable solution to the needle-less injection device. The injection test shows that the device is capable of injecting a known volume of drug in the fatty tissue of pig skin. Prototype 1 also showed some of the problems with the device and provides insight for future improvements.

5.6 Testing conclusions

Successful injections were achieved with Prototype 1 showing that the device is capable of injection into pig skin. The injections shown in Section 5.4.1 are approximately 1 to 2 mm below the surface of the skin. This region of tissue is acceptable but a deeper injection into the fatty tissue and inter-muscular tissue is more desirable. Because of the differences in the model tissue and human tissue, it is expected that equal or greater depths would be achieved with this prototype if injecting into human skin

The injections were not always successful and many times there was leakage around the nozzle. This is most likely due to insufficient injection pressure and too much drug volume which causes leakage around the nozzle. The injection success was highly dependent on the skin thickness, freshness and type. Many times an injection in an area of skin would not work, but when using the same parameters in another area of the same piece of skin, the injection was successful. This observations leads to the idea that the injection pressure and speed were very close to the minimum needed to penetrate skin. For a more robust design, the speed of injection should be increased so that the injections are deeper in the skin.

The energy requirements were very close to the predicted value of 61 J and were low enough to make the device viable showing that the limited actuation efficiency of NiTi is not a significant issue. The energy usage of less than 100 J is well below the energy contained in a 0.1 kg battery alkaline battery which is 35000 J.

5.7 Design Requirements conclusions

Prototype 1 was a successful test of the basic concept and some of the requirements that will be used in the final design. The prototype shows that a compact device using NiTi for actuation, can successfully be used as a needle-less injection system.

5.8 Notes for further revisions

Prototype 1 worked well as a prototype of a hand held needle-less injection system. The device however had several flaws that were changed in further design studies. Although the device was handheld, a more stable platform for testing would be desirable to get more data. The device was over built with heavy parts which could have slowed the acceleration of the piston. Finally the drug vial was a part of the system and should be made a separate part which can be interchanged. The design recommendations were taken into account when designing Prototype 2.

6 Prototype 2

6.1 Prototype 2 design goals

Prototype 2 was designed to obtain quantitative measurements for the various parameters tested. The prototype setup is modular and capable of measuring many of the injection parameters such as fluid speed, piston position, skin contact force and drug pressure. The goal for this design was to achieve an understanding of the system and tune the device to perform more reliably. Prototype 2 was also designed to have variable parameters so that changes in nozzle design or piston diameter could be made with no redesign. Although this was a measurement prototype, some of the overall design criteria were implemented in the device, such as removable drug vials and size requirements.

Prototype 2 was created using the same basic design as Prototype 1, however the device was changed from hand-held to a table top device. This change was made for testing purposes and provides a stable test setup. Additional sub-systems were created to measure the desired parameters.

Prototype 2 improves upon the wire tensioning method and electrical contact design from Prototype 1. The original prototype has a wire tension method in which each wire was individually tensioned. Equal tension in each of the wires was hard to obtain and it was difficult to attach the electrical wires to the contacts. The motion of the original prototype although already smooth was improved in Prototype 2 using linear bearings. The weight of the individual components such as the piston and pusher were reduced to lower inertial effects.

The table top design for Prototype 2 is shown in Figure 6-1 with the components described above.

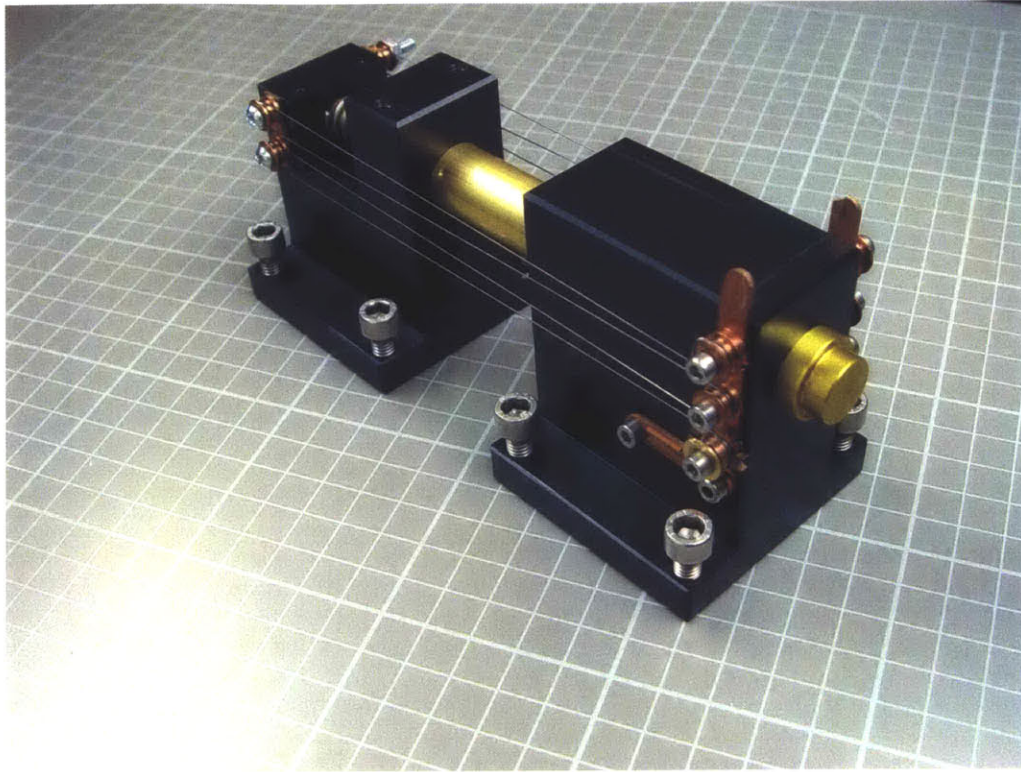


Figure 6-1. Injection device module.

6.2 Design Criteria for Prototype 2

The design criteria were developed to facilitate the design of a test setup capable of quantitative measurements of the injection parameters. Requirements were further obtained from the overall device requirements. The central design criteria for Prototype 2 was to develop a small, modular measurement setup with removable drug vials.

The device needed capabilities of measuring the fluid speed, piston position, skin contact force and drug pressure. Figure 6-1 is a schematic showing the various testing parameters. Injection success was also preformed by observation of the depth of penetration.

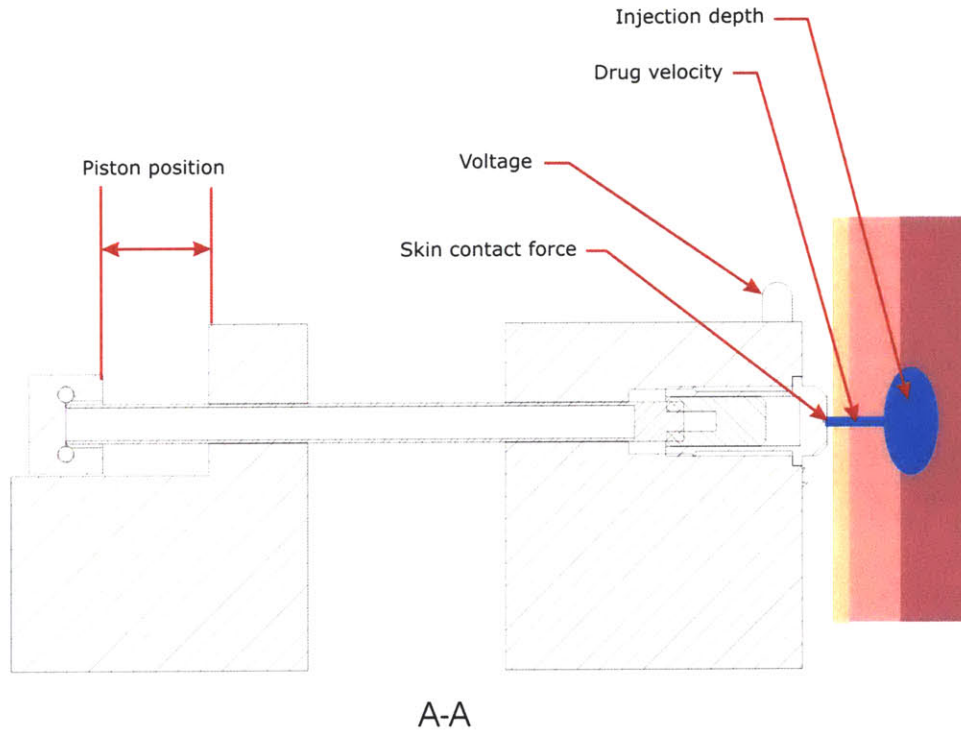


Figure 6-2. Measurements performed using Prototype 2.

To facilitate the ability to conduct different tests using the same test setup modularity was added to the requirements. Prototype 2 was constructed of individual test modules which could be interchanged for different tests as needed. An optical table was used as the bread board due to its uniform hole spacing and precision.

Prototype 2 has many of the same design criteria as Prototype 1 such as drug volume, length and actuator method and type. The hand-held requirement was removed due to the need for a stable device to conduct tests.

The device was designed with a removable drug vial which allows for a greater diversity in nozzle and piston design. It also implements the overall device requirement for disposable, removable drug vials.

In addition to these requirements, Prototype 2 was designed as an improvement of Prototype 1. Problems noticed in the original prototype were corrected during the design process for Prototype 2. An improved tensioning system was designed as well as improved piston motion. Contacts were redesigned to provide a better connection to the power source.

Table 6-1 shows the design requirements for Prototype 2.

Table 6-1. Design requirements for Prototype 2.

Criteria	Description
Size	Optical Table design
Length	150 mm
Height	50 mm work height
Overall design	Modular
Life	Multiple Use
Construction	Robust
Actuation	NiTi wire
Actuation method	Joule Heating
Drug Volume	up to 500 μ L
Vials	Removable

6.3 Components

Three main modules comprise Prototype 2: the device, testing equipment, and the housing. The design procedure for this device was first to make a preliminary design of the parts. Once the concept for the components was made, basic engineering design was applied to each of the components to develop a working device. The components were then solid modeled in SolidWorks2001 [16].

6.4 Injection device

The injection device is similar to the first prototype with several modifications. The main components have not changed and are as follows: the body, pusher, drug vial and NiTi actuator. These components comprise the working injection device and are considered a single module in the test setup.

6.4.1 Overview of basic layout

The overall device is shown in Figure 6-3 and the various components of the device are indicated. Each component is explained in further detail in the following sections.

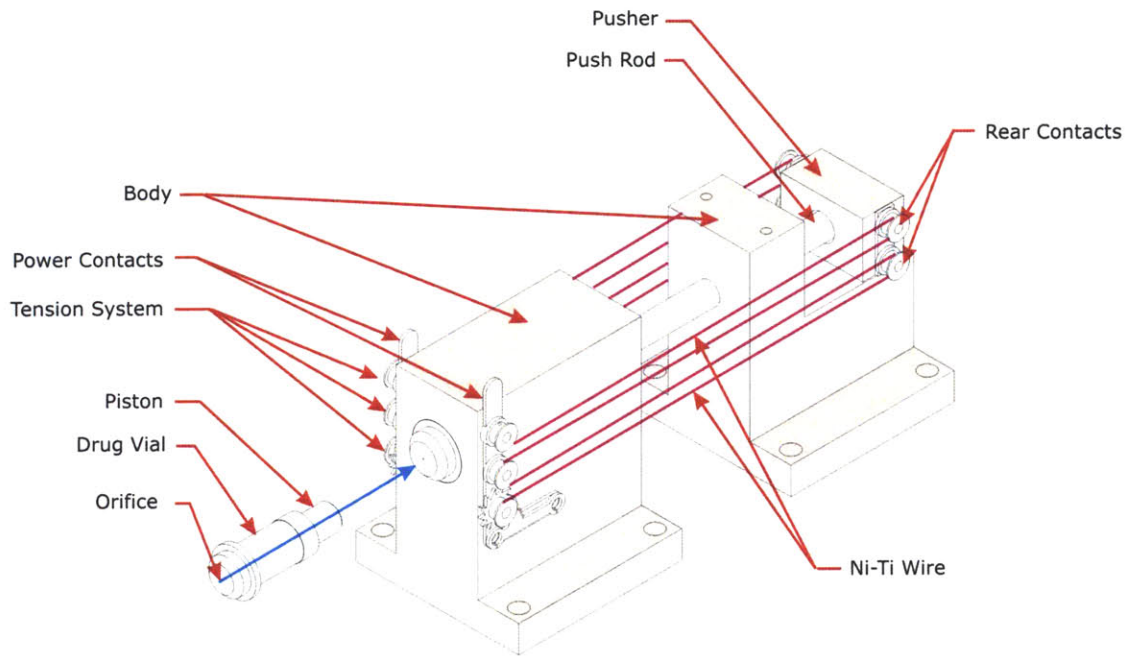


Figure 6-3. Injection module.

6.4.2 Body

The body houses a drug vial and provides the bearing surface for the pusher piston to inject the drug. All the other components in the injection device interact with the body.

The base provides the working height of 50 mm. All of the modules in this setup were designed with a working height of 50 mm from the optical table surface. This provides a uniform working area so that parts could interact easily. The base is separated into 2 parts which can be placed at various lengths to increase or decrease the device length. The body has bolt hole spacing of 50 mm so that it easily fits on the optical table setup. The standard length for the device was set at 150 mm by placing the separate base parts at appropriate distances on the optical table length can be changed. Linear bearings were added to the body parts to decrease the friction of the push rod.

The drug vial was designed to screw into the body. This decision was made to simplify the design while making the vials removable and interchangeable.

6.4.3 Pusher

The piston in Prototype 2 differs from the one used in Prototype 1. In Prototype 1 the piston was attached to the NiTi and was directly linked to the drug volume. In Prototype 2 the piston is much shorter and is contained in the drug vial component. This allowed for the use of different sized drug vial piston combinations. A second permanent piston was designed in Prototype 2. This piston, known as the pusher, was attached to the NiTi and contacts the drug vial piston for injections. Figure shows the Prototype 2 piston arrangement. The NiTi is attached to the body at the front and attached to the pusher in the back.

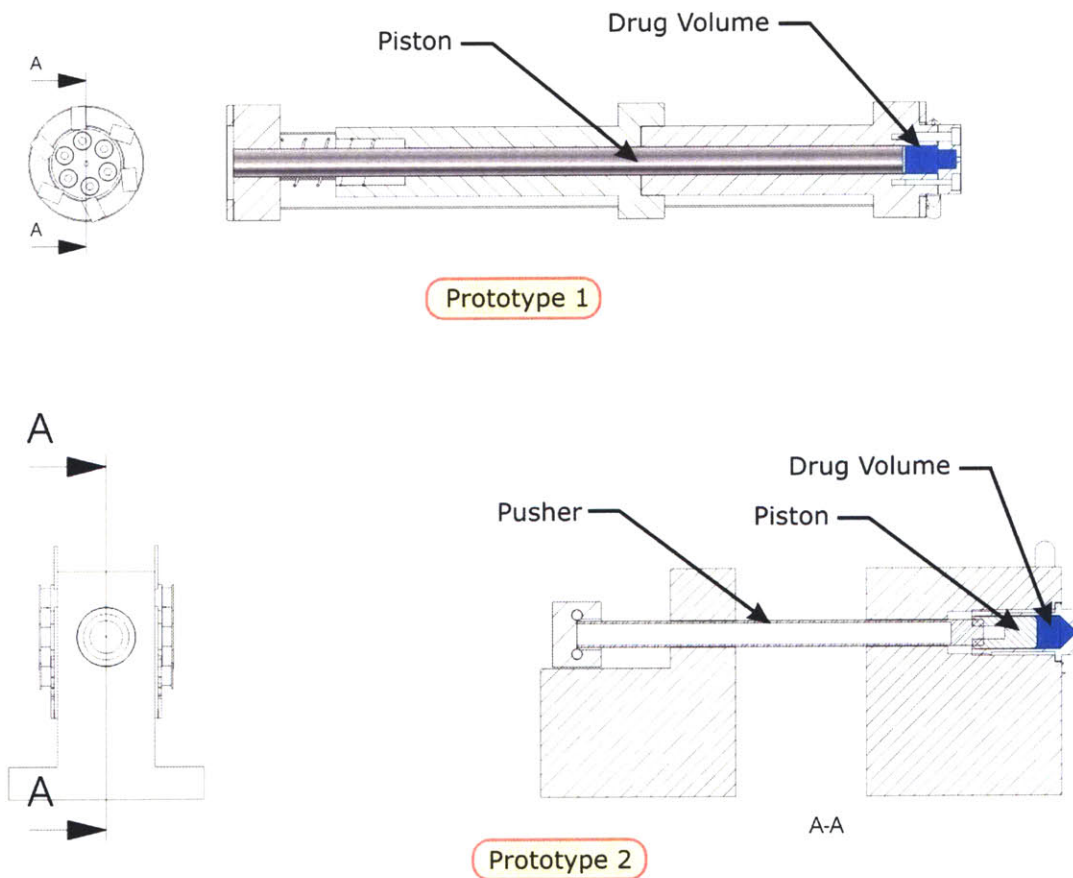


Figure 6-4. Comparison of piston arrangement for Prototypes 1 and 2.

In this configuration the push rod slides on the bearing surfaces made in the body and contacts the drug vial and piston. The pusher is made of two main parts: the push rod and the push block.

The push rod was constructed from aluminum hollow rod to reduce weight there by its inertia. The push block was constructed of Delrin (machinable poly-acetal) also to lower the weight. The NiTi wire is attached by the contacts which will be discussed in Section 6.4.5. The pusher was designed to be lightweight and have the necessary stiffness so it would not buckle under the forces exerted by the NiTi. Figure 6-5 shows the dimensioned drawings of the two main parts.

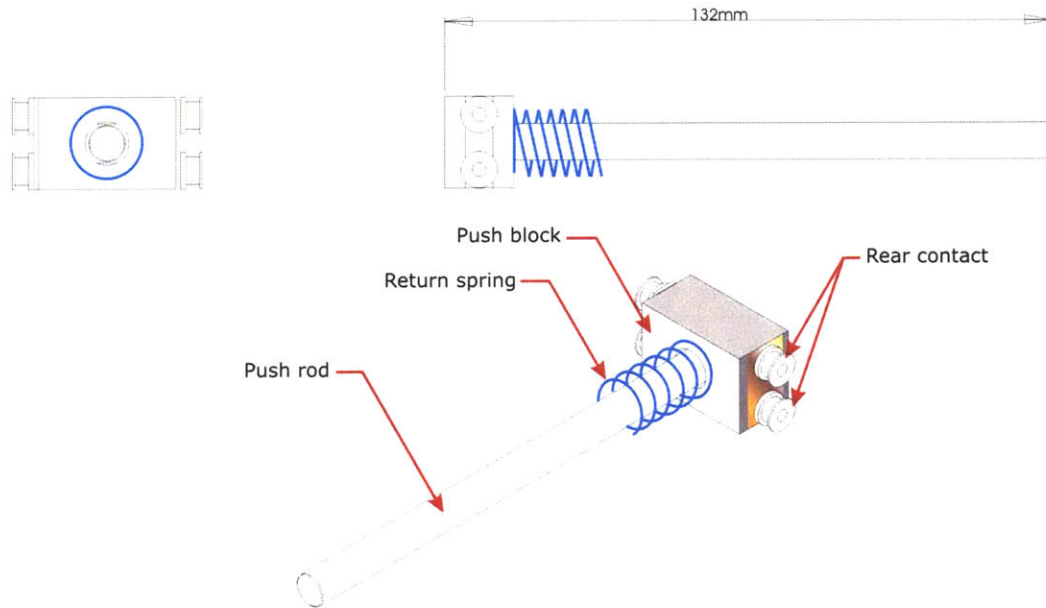


Figure 6-5. Solid model of pusher rod used in Prototype 2

It can be seen in this figure that a return spring was added to provide tension on the NiTi wire when in its fully extended state.

6.4.4 Drug Vial

The drug vial was designed as a completely separate part from the injection device thus making it more like the desired final product. The drug vial was designed to be fully functional and has the basic components for injection: the drug volume, piston and nozzle. Interchangeable drug vials were constructed with various orifice diameters and piston diameters. Figure 6-6 shows the solid model of the drug vial.

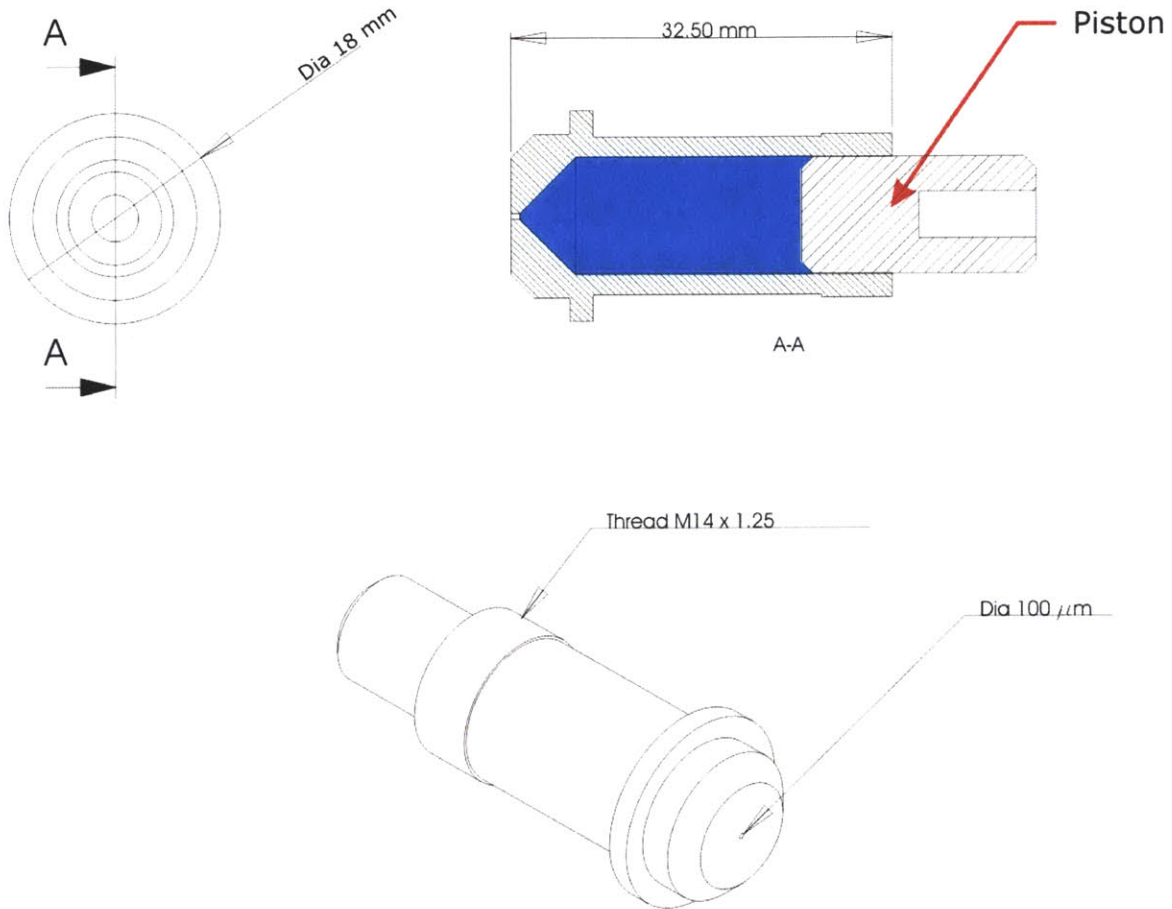


Figure 6-6. Solid model of drug vial and piston

The drug vial was constructed from aluminum. Unlike Prototype 1 which uses a needle as the orifice, a hole was drilled in the drug vial nozzle. By drilling the hole directly into the body of the drug vial the assembly steps were reduced. The length of the orifice is approximate 500 μm and the diameter ranged from 80 μm to 200 μm . Several drug vials were made with different orifice diameters.

By making a separate drug vial which contains the piston, the amount of drug injected could easily be changed by varying the piston diameter. This also changes the pressure provided by the NiTi wire. The force that the wire generates when contracting remains constant but the area over which the force acts is varied by changing the piston diameter. Completed drug vials are shown in Figure 6-7.



Figure 6-7. Drug vials for Prototype 2.

The piston was made of precision ground drillstock. Drillstock was chosen for its high tolerance and provided a close fit with the piston cylinder. The clearance was approximately $50\ \mu\text{m}$ to $100\ \mu\text{m}$.

6.4.5 NiTi wire

As in the first prototype, NiTi wire was used as the actuation method. The wire used in the prototype was $380\ \mu\text{m}$ in diameter and is attached to the device by winding the wire around pulleys. The pulleys act as the capstans in Prototype 1 and hold the wire in place. This design eliminates the need for multiple tensioning units for each wire. One tensioning unit was placed on either side of the device and controls the tension of all the wires on that side.

Instead of six wires arranged in a circle around the device as in the first prototype; the arrangement was changed to two rows of four wires on each side of the device. A tensioning ratchet was used to tighten the wires and is shown in Figure 6-8. A compression spring was added to the pusher to keep the tension when the device was not in use.

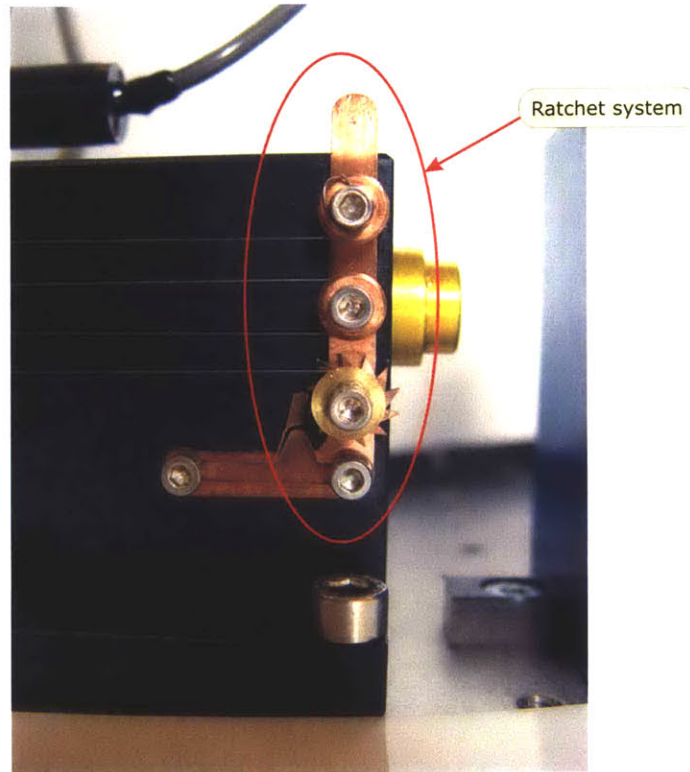


Figure 6-8. Ratchet tension system for Prototype 2.

Having the wires wound around pulleys evened the tension in the wires any remaining slack in the NiTi on either side could be adjusted using the tensioner.

6.5 Testing Components

Testing modules were used for various measurements and were designed and added to the setup as needed. The desired measurements were as follows: piston position measurement, stream velocity measurements, skin contact force, actuation current and voltage and drug pressure to stream velocity measurements. Each of these tests required different setups. Most of the measurements were conducted on the injection device module except the drug pressure and velocity test which was conducted using the pressure vessel module.

6.5.1 Voltage and current

As the capacitors discharged into the NiTi wire causing them to heat, the voltage on the capacitors decreased. This voltage was measured using a Tektronix oscilloscope (model 2014) attached to the contacts [17]. The voltage measurements were the first and

simplest test conducted on the apparatus. The measurements can be used to find the approximate energy dissipated in the system during a injection using the Equation 6.

The exact energy used could not be found in the current setup because the resistance of the NiTi varies during the contraction. However the resistance does not vary significantly.

6.5.2 Skin Force Measurement

The injection device must be placed against the skin with sufficient force to maintain a seal with the skin while the injection takes place. To find the force required for proper injection, measurements were taken using an Extech force gauge (model 475040) shown in Figure 6-9 [8].

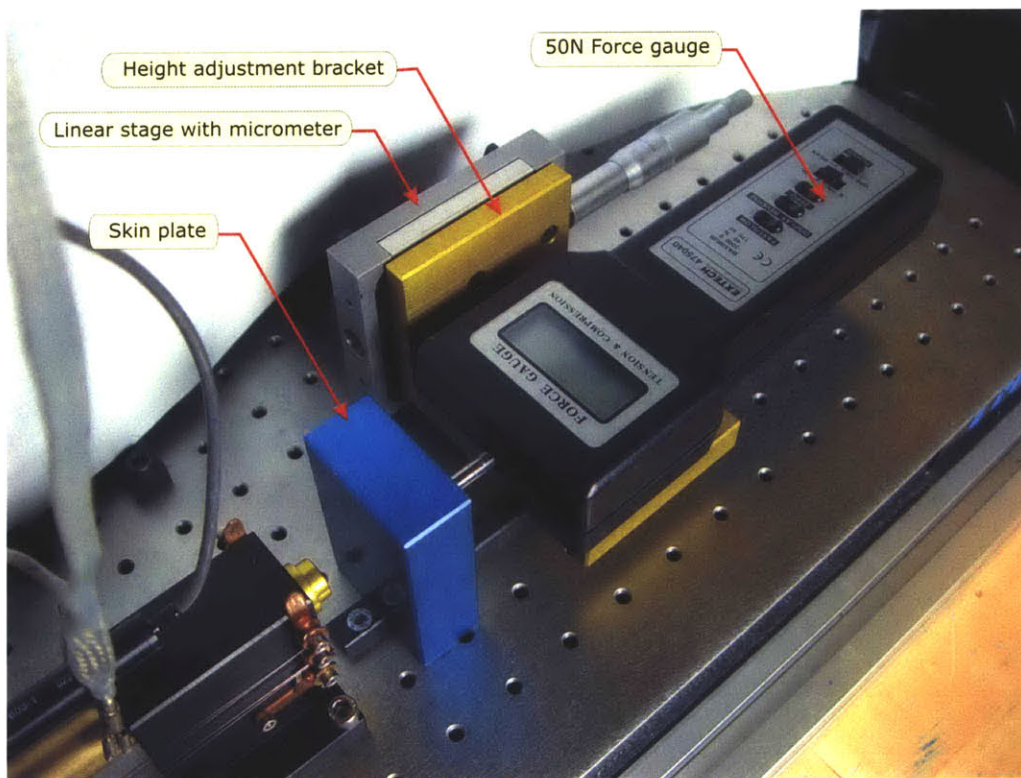


Figure 6-9. Force gauge module used for skin contact force.

This module was design to force the skin against the nozzle for the injection; it includes a linear stage attached to the force gauge. The force gauge contacts the skin plate and can apply the necessary force against the plate for injection. This setup allows for measurements to be taken without placing any measurement device near the injection

site. The force gauge centerline was placed at 50 mm from the table base for the proper working distance.

6.5.3 Drug vial position measurement

To find the acceleration, velocity and position of the piston, a measurement module was added to the setup. This module consisted of a linear potentiometer (Omega, LP803-1) and a connection system shown below in Figure 6-10. This potentiometer has a resolution of 127 μm .

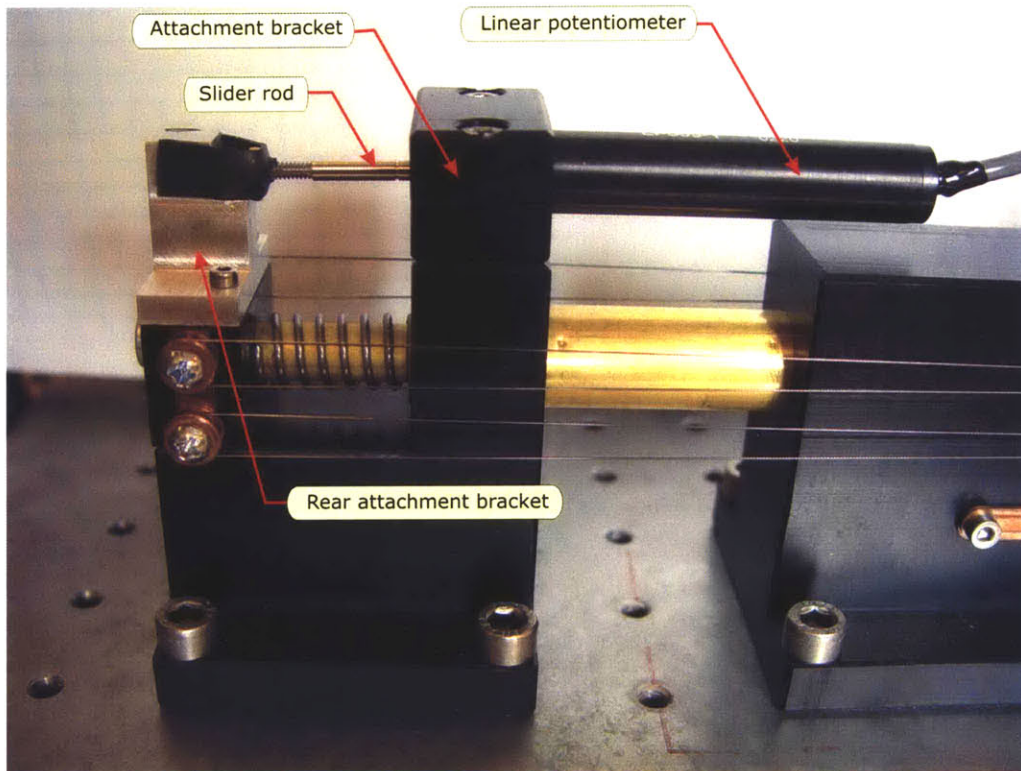


Figure 6-10. Position sensor module.

The position module is shown attached to the body of the drug injector. The potentiometer was supplied with a 10 V source and the output voltage was measured on a second channel of the oscilloscope.

A calibration test was performed using a linear micrometer to move the potentiometer a known distance and measuring the voltage change. A plot of position with respect to voltage is shown in Figure 6-11.

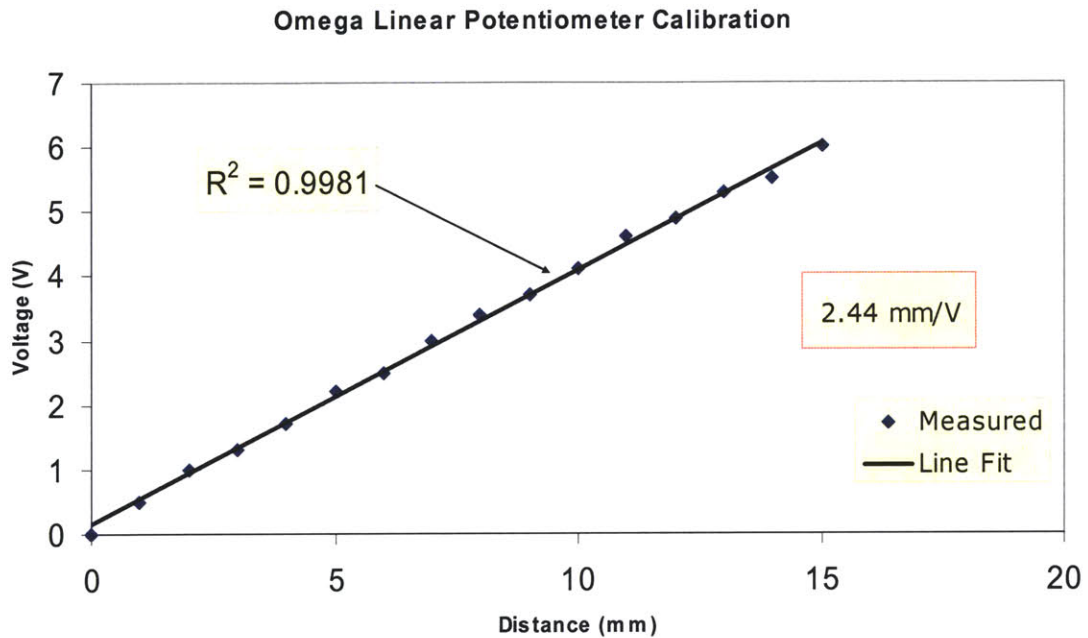


Figure 6-11. Calibration plot for the Omega linear potentiometer (the variance accounted for, R^2 , by the fitted line also shown).

The position measurement was taken with respect to the injection device body, which was mounted to the optical table. The arm of the potentiometer was connected to the pusher. Changes in the piston position were directly related to the potentiometer voltage by the relationship 2.44 V/mm. A typical measurement recording from the position module is shown in Figure 6-12.

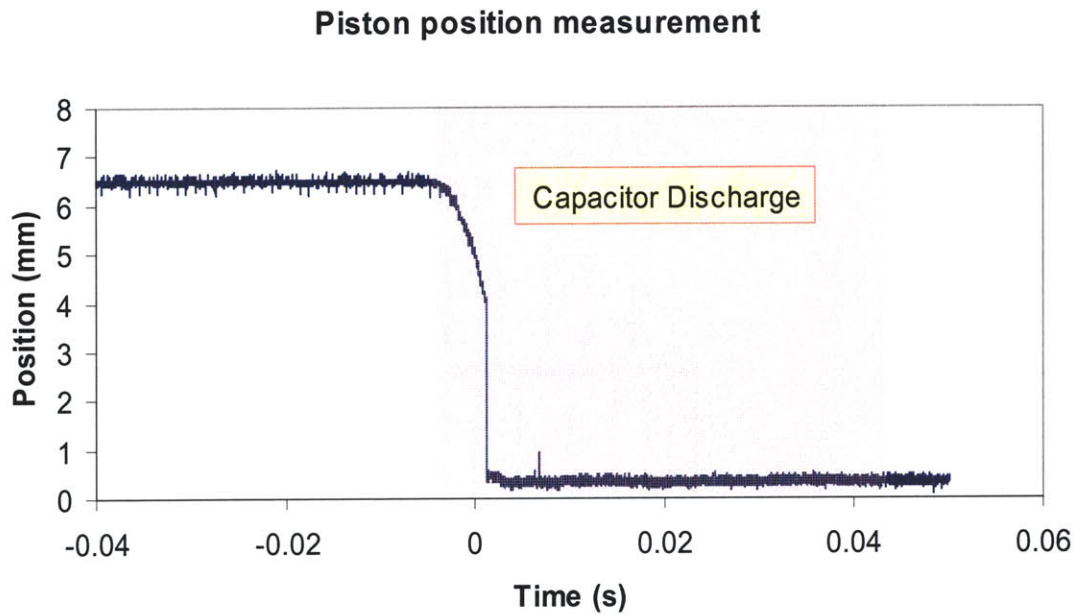


Figure 6-12. Typical recording from the position module.

6.5.4 Drug Velocity

The drug velocity, which relates directly to injection depth, was measured using a break beam setup. This module consists of 2 break beam sensors attached to the Tektronix oscilloscope and a power source. Figure 6-13 shows a schematic of the setup.

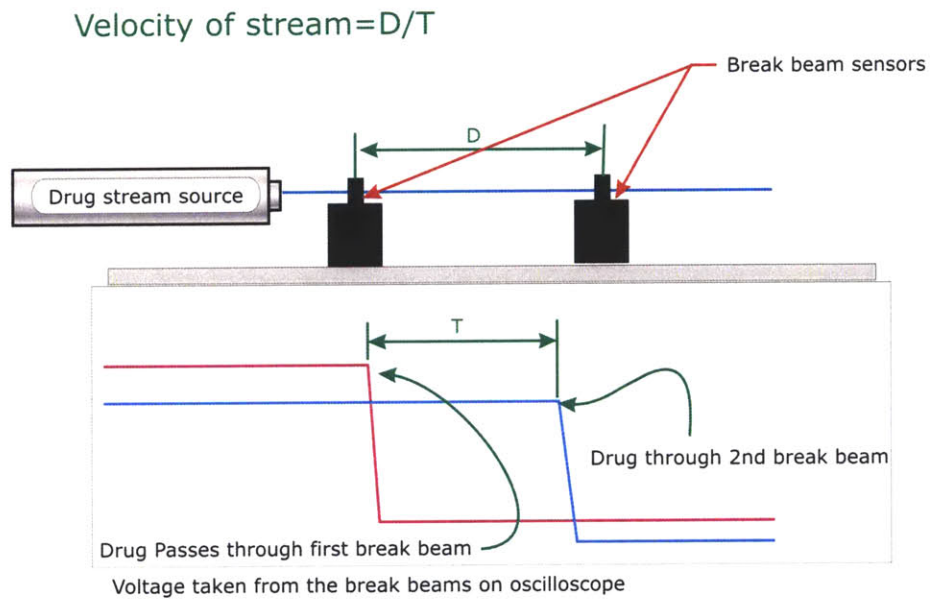


Figure 6-13. Schematic of the break beam setup.

The break beam module measures the time for a stream of drug to travel a known distance thus yielding the velocity. The sensor shown in Figure 6-14 is a break beam sensor which when supplied with a voltage yields a voltage change as the drug stream passes through. The voltage sampling rate was 10 MHz. For velocities in the range up to 250 m/s the velocity errors due to sampling was $\pm 0.2\%$.

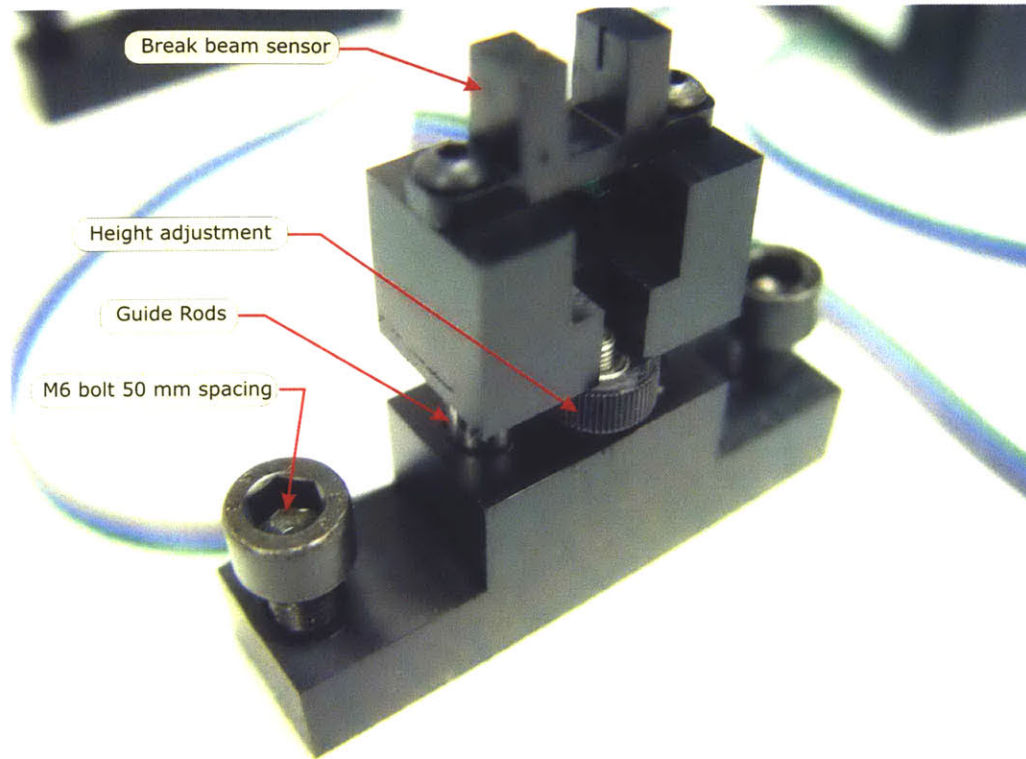


Figure 6-14. Break beam module.

As the beam passes through each break beam sensor, a pulse is recorded. By dividing the distance by the time difference between the two pulses, the average velocity is found. A typical recording from the oscilloscope is shown in Figure 6-15 along with the critical features shown.

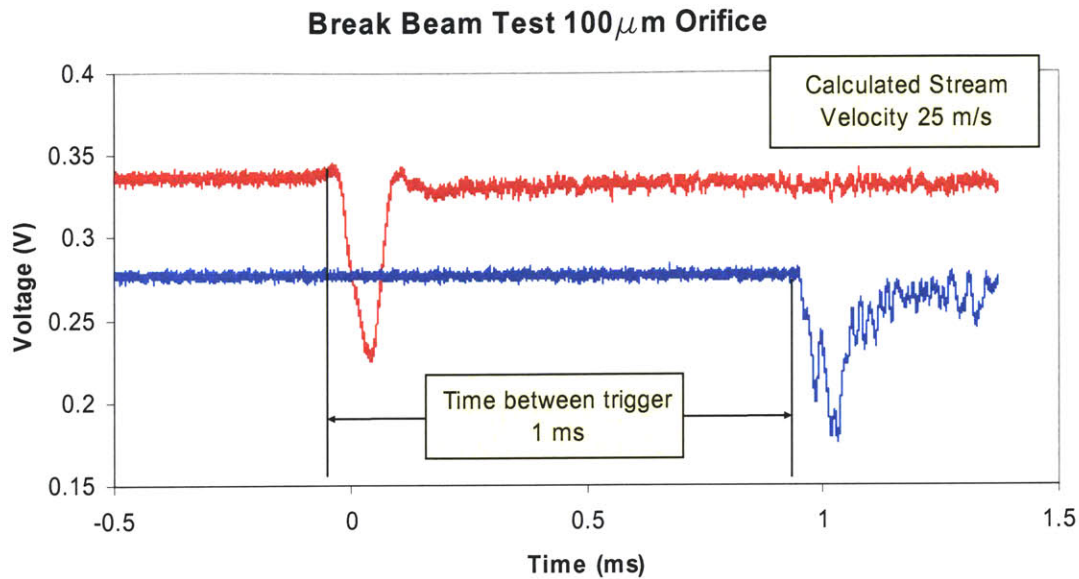


Figure 6-15. Break beam module recording.

The voltage change is approximately 30% of the total voltage which is a large enough change to trigger the device.

6.5.5 Drug pressure velocity measurement

As the results and testing will show in the following sections, the theoretical pressures achieved during injection did not match the predicted velocities. In order to discover what pressures were required to achieve a given velocity, a secondary device was constructed to measure the relationship between pressure and velocity for a drug vial. This device uses the same drug vials as the actual device but used pressurized Nitrogen as the actuation method. The device shown in Figure 6-16 acts as a pressure vessel and accepts a standard drug vial.

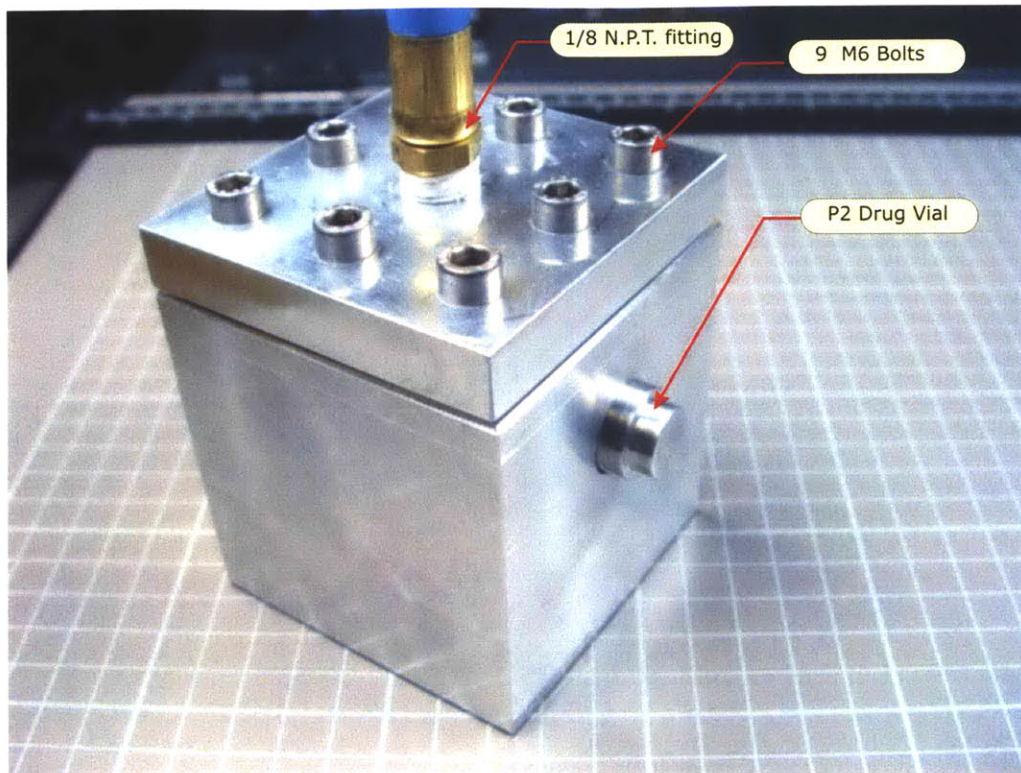


Figure 6-16. Pressure vessel used in pressure velocity experiments.

The drug was placed in the vessel and sealed. As pressure was supplied to the vessel, the drug was expelled through the orifice. A stainless steel shim stock was placed in front of the orifice, acting as a shutter. The shutter was raised and lowered manually to obtain pulses. The break beam module was used to measure the drug velocity. The pressure was varied by a regulator on the Nitrogen line and was measured using a gas gauge. The overall setup is shown in Figure 6-17.

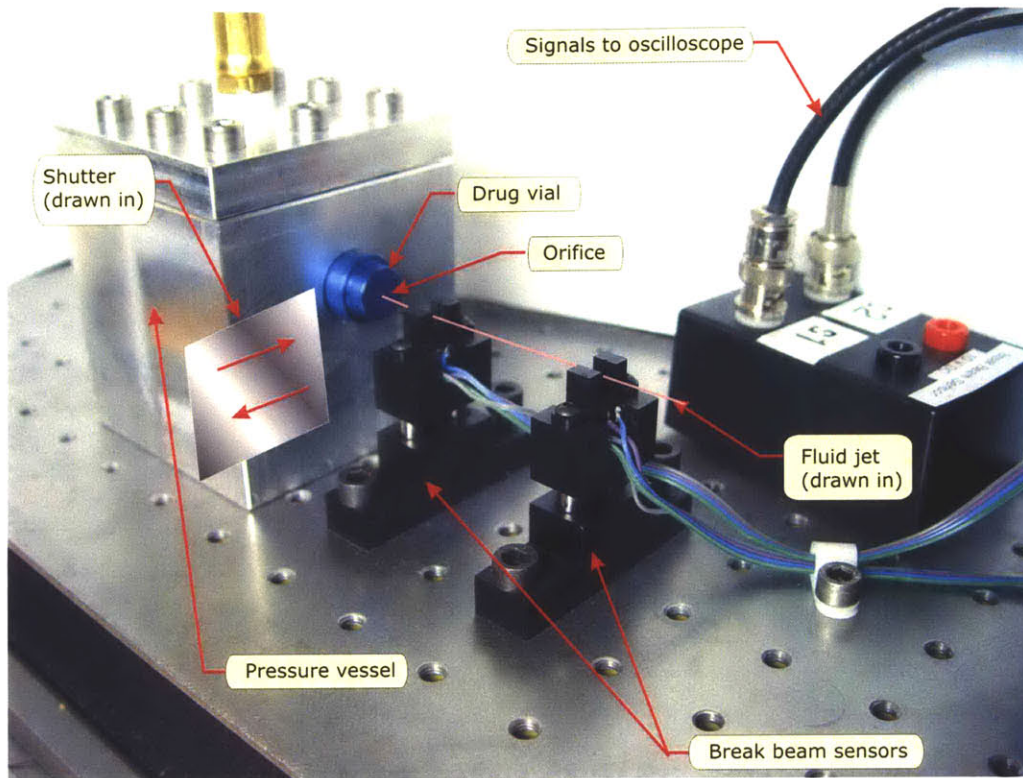


Figure 6-17. Pressure velocity experimental setup.

6.5.6 Setup Housing

The housing was constructed using MK extrusions for a clean setup where the apparatus could be easily viewed. The instruments were placed on a rack above the work area and Plexiglas was added for safety. The housing was modeled in SolidWorks2001 and is shown in Figure 6-18.

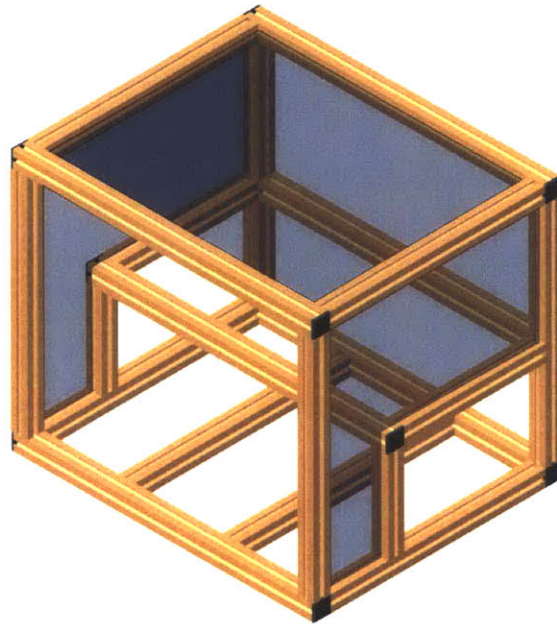


Figure 6-18. SolidWorks 2001 model of MK housing.

This cage was then constructed using the MK extrusions and links, which provided a solid, sturdy setup.

Testing was conducted by placing the various modules in different configurations to produce the different steps. Each of the configurations will be shown in detail in the following sections.

6.6 Testing and Data

6.6.1 Injection test

The goal of this test was to determine the required piston diameter and drug volume to obtain injection success. Injection was tested on shoulder skin from a pig. The test measured injection depth, piston position profile, voltage profile, and skin contact force. Approximate energy dissipated, injection volume and drug speed were also calculated from the raw data. The piston diameter was varied from 2 mm diameter to 10 mm diameter. Table 6-2 shows the piston diameters used as well as the drug volume contained and the theoretical pressure generated during the injection.

Table 6-2. Piston diameters used in the injection tests.

Piston Diameter (mm)	Volume (μL)	Theoretical Pressure (MPa)
2	21	57.8
6	280	6.42
10	550	2.31

The injection depth was measured by visual inspection of the injection site. A scalpel was used to cut the skin in sections allowing the depth of penetration to be examined. The dye used was Coomassie blue which stains protein and provides good color for visual inspection.

The piston position was measured using the position module attached to the Tektronix oscilloscope. The voltage profile was also measured on the oscilloscope. The force measurement was conducted before the injection by positioning the skin close to the nozzle and applying force using the linear stage to move the skin into contact with the nozzle.

The energy dissipated during the injection was found using Equation 6 which relates the voltage profile to the energy dissipated. A constant injection time of 250 ms was used to accommodate different contraction times. The energy dissipated was calculated by integrating over the time it took for the piston to contract. Injection volume was found by calculating the total displacement of the piston from the position module and the cross-sectional area of the piston using,

$$Vol = Lc * Apl . \tag{7a}$$

The position module was also used to measure the approximate drug speed. The volume of drug was divided by the piston contraction time to obtain the volume flow rate (Q). The volume flow rate was divided by the orifice cross-sectional area to obtain the drug velocity,

$$\dot{Q} = \frac{Vol}{T} , \tag{7b}$$

$$V = \frac{\dot{Q}}{Acc} . \tag{7c}$$

The test setup is shown in Figure 6-19 and lists the modules used during the injection test.

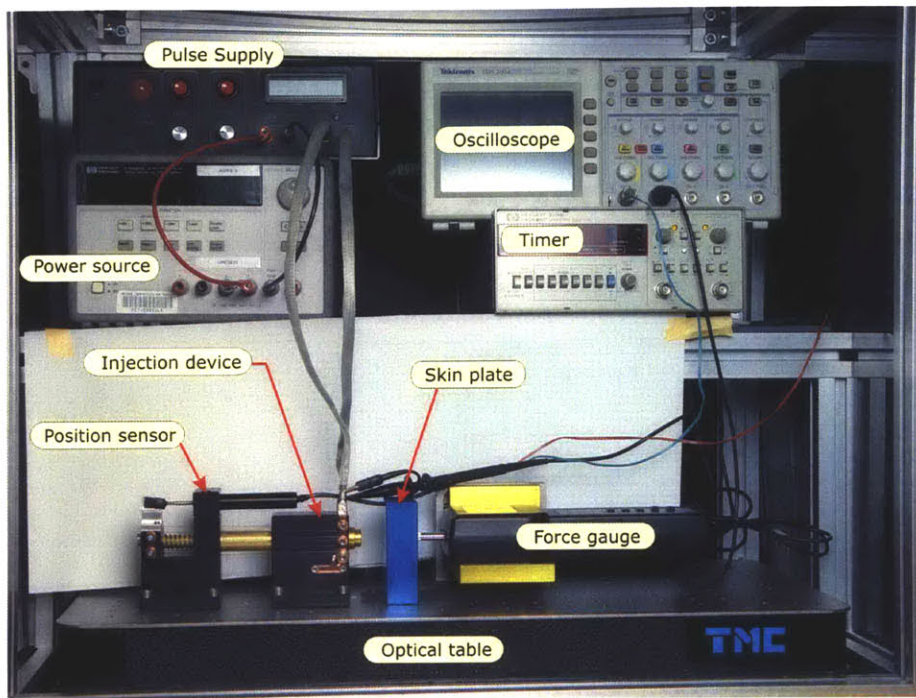


Figure 6-19. Test setup for injection test.

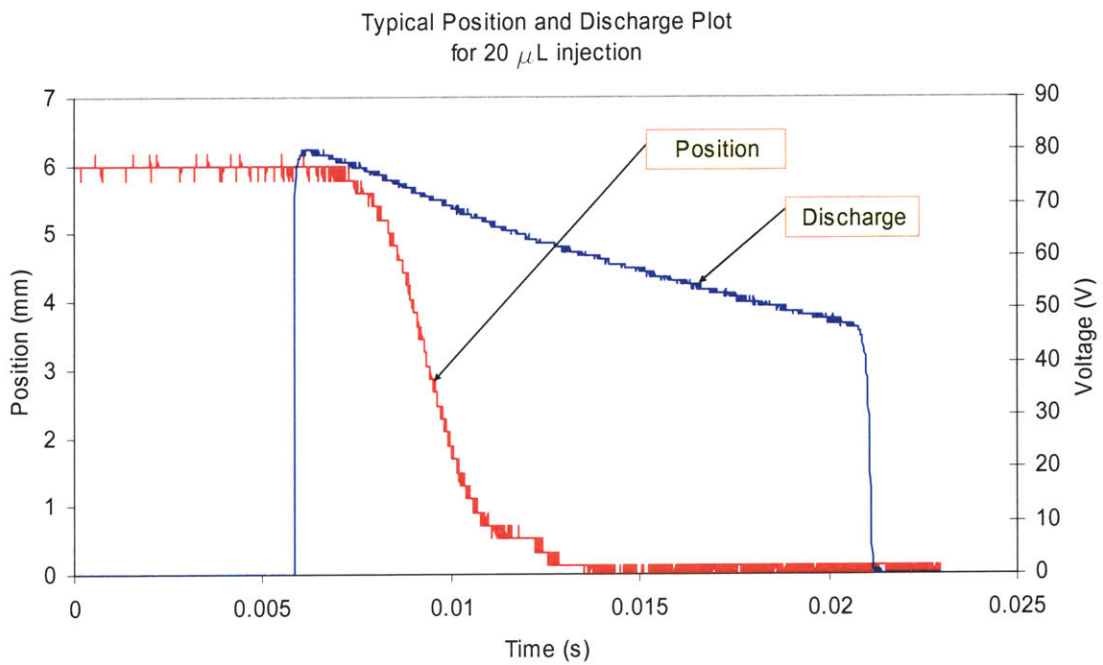


Figure 6-20. Typical injection test conducted with 2 mm drug vial.

Figure 6-20 shows an example of a piston position profile and voltage profile. In this experiment, the capacitors (0.048 F, 100 V) were charged to 80 V. The energy dissipation during this 15 ms pulse was 85 J. The position profile for a 20 μL drug injection resulted in an average drug speed of 240 m/s over the injection time. The measured skin contact force was 1.5 N. Figure 6-21 shows the before and after view of the skin in several orientations. The injection depth was approximately 5-10 mm.

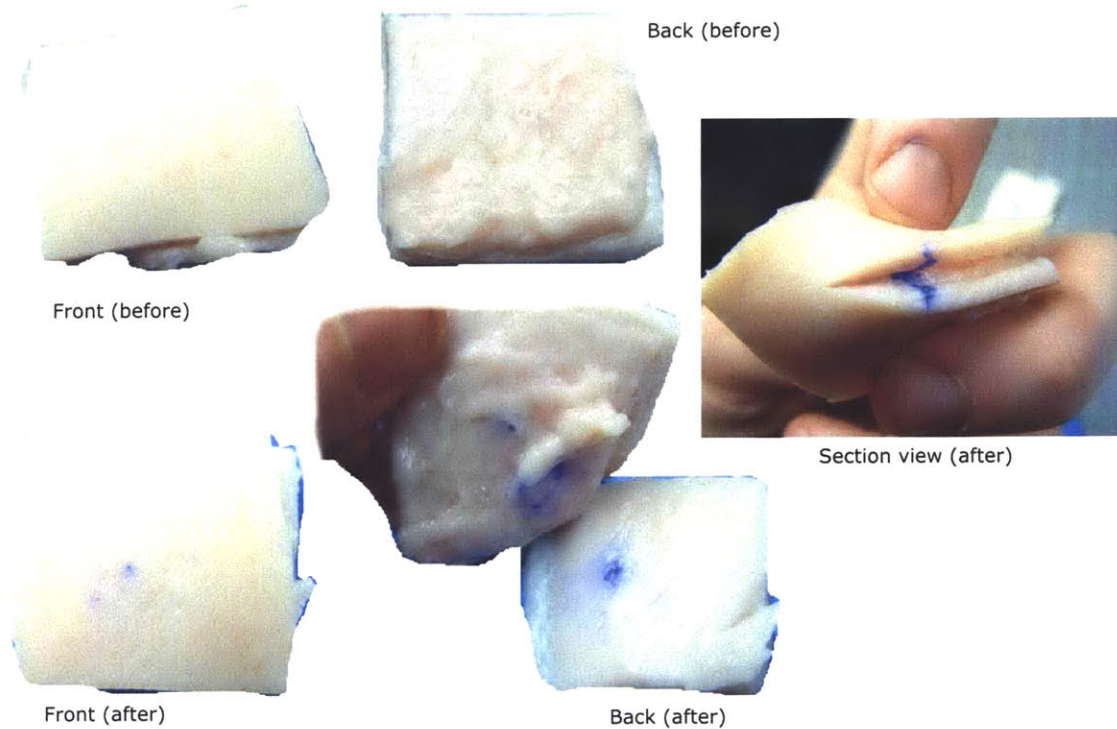


Figure 6-21. Photo of pig skin before and after injection.

Tests were conducted using the three different drug vials and are shown in Table 6-3 with the measurement data.

Table 6-3. Measurement results for injection test.

Piston Diameter (mm)	2 mm	6 mm	10 mm
Contraction length (mm)	6	5	5
injection time (ms)	11	20	1000
Skin contact force (N)	1.5	1.5	1.5
Injection depth (mm)	7	1	0
Injected volume (μL)	19*	141*	392*
Injection speed (m/s)	240*	90*	50*
Energy required (J)	30*	189*	195*
Notes	Injection was successful	Some success leakage occurred	no success

***Calculated Values**

The measurements show that injections using a 2 mm drug vial were successful while the 6mm drug vial had marginal success and the 10 mm drug vial had no success. The measured drug speed for each of the vials shows that the large vials were below the 100 m/s initial design goal while the 2 mm vial was much higher. The energy required and the injection time was smaller for the 2 mm vial.

The capacitors were varied from the 50 V 0.156 F to the 100 V 0.048 F bank. This was done to increase the power delivered in an attempt to increase the injection speed. The larger capacitors can deliver a higher current and therefore will heat the wires more quickly. Injection measurements taken with this larger capacitor bank are shown compare to the initial tests conducted with the 50 V capacitors in Table 6-4.

Table 6-4. Comparison of injection tests done with different capacitors.

Piston Diameter (mm)	Contraction length (mm)	injection time (ms)	Energy required (J)	Injection speed (m/s)
2	6	11	30*	240*
2	6	8	56*	300*

***Calculated Values**

Table 6-4 shows that the larger capacitors, while supplying more energy, have little effect on the overall contraction time. A possible explanation for this observation is that the strain rate of the NiTi alloy for the given load may have been reached. The strain rates in these experiments are approximately 4 s^{-1} which may be the maximum rate for the pressure required.

6.6.2 Drug Velocity

In Section 6.6.1 the measured calculated velocity for each of the drug vials was obtained. These values, however, do not match the theoretical drug speeds that should have been obtained given the theoretical pressure generated during injection. Table 6-5 shows the predicted drug speeds based on pressure and the calculated drug speed from Section 6.6.1.

A drug velocity experiment was conducted to obtain measured values for the drug speed for each of the drug vials used. The experiment was conducted using the injection device module and the break beam module. The experimental setup is shown in Figure 6-22.

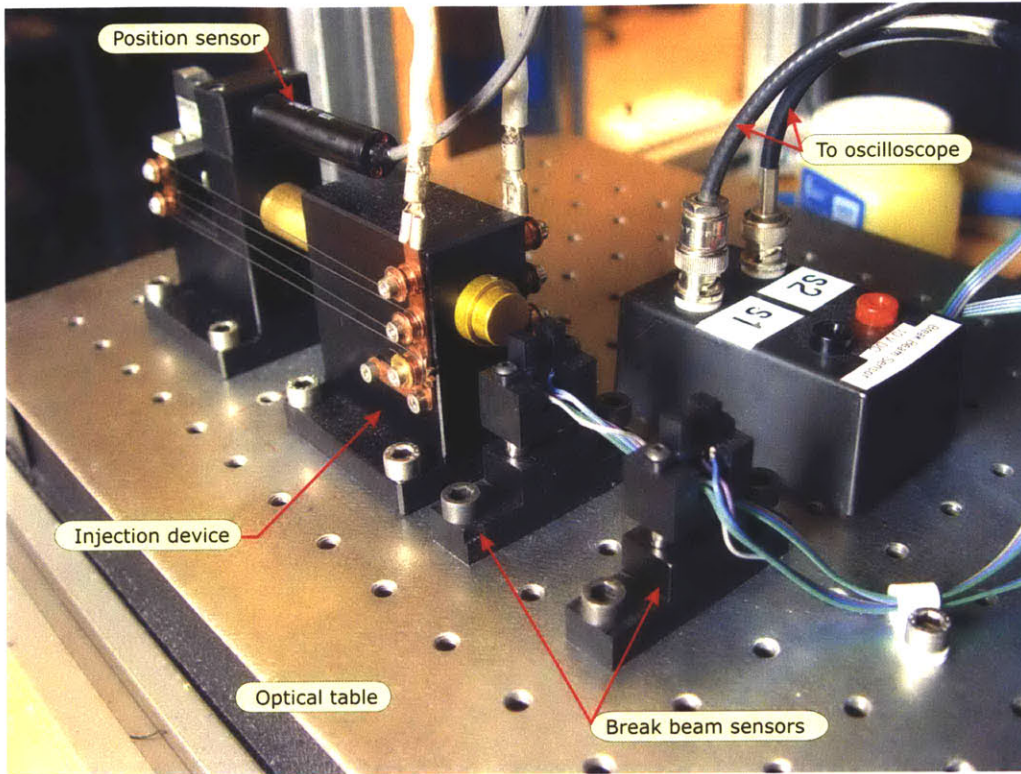


Figure 6-22. Experimental setup for drug velocity measurements.

The results of the experiments are shown in Table 6-5 along with the theoretical and calculated velocities. The data shows that the velocities measured are much less than the theoretical values.

Table 6-5. Comparison of the measured, theoretical and calculated velocities.

Piston Diameter (mm)	Measured Velocity (m/s)	Calculated Velocity (m/s) from piston position	Theoretical Velocity (m/s)
2	160	240*	760
6	65	90*	242
10	25	50*	140

* Calculated Values from piston position measurement module

There were two possible causes for this difference in velocities. The pressure generated by the NiTi could be much less than the theoretical value or the turbulent flow equation used to predict the pressure drop could be yielding results which are not applicable to this geometry and size. To determine the source of the discrepancy in the pressure-velocity relationship, velocity tests were conducted on the drug vial.

6.6.3 Pressure Velocity measurements

The pressure-velocity measurements were conducted using the pressure vessel and the break beam modules. The pressure was varied from 400 to 1700 kPa while measuring the stream velocity. The maximum pressure was limited to 1700 kPa by the regulator limits. It was observed that a pressure greater than 1700 kPa was required to achieve the desired fluid speed. Figure 6-23 shows the stream velocity as a function of pressure.

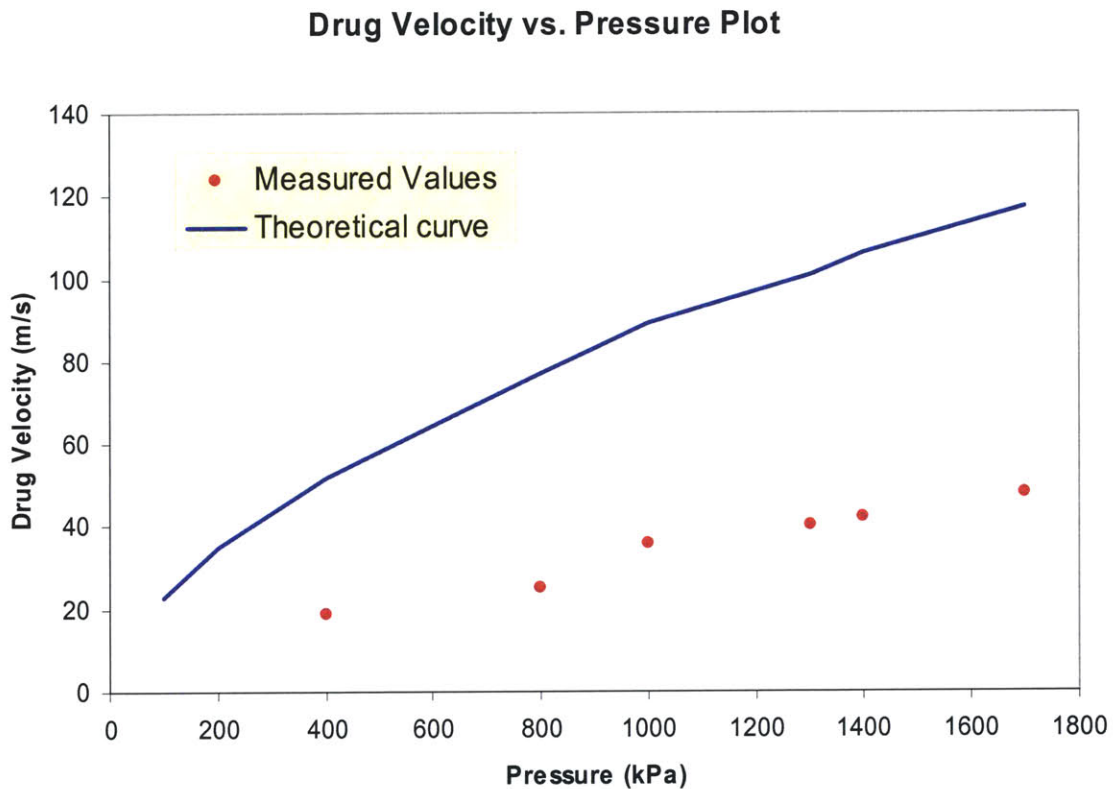


Figure 6-23. Stream Velocity as a function of pressure

From the curve above it can be seen that the velocity resulting from a given pressure is lower than that predicted by the turbulent flow equation. A linear fit of the data yields the pressure-velocity relationship,

$$V(P) = 2.31 \times 10^{-5} (P) + 9.537. \quad 8$$

This equation however cannot be verified at pressures above 1.7 MPa that occur during injection.

6.7 Test measurement analysis

From the data collected from the velocity-pressure measurements, an optimal piston diameter was found for the given setup and design geometry. Given a $100\ \mu\text{m}$ orifice and a 7.5 mm contraction length the optimal piston diameter would be between 3 and 5 mm shown in Figure 6-24. It is expected that the drug speeds for piston diameter in this range would be between 100 m/s and 200 m/s. Table 6-6 lists the drug volume contained in 3, 4 and 5 mm drug vials and the predicted speed.

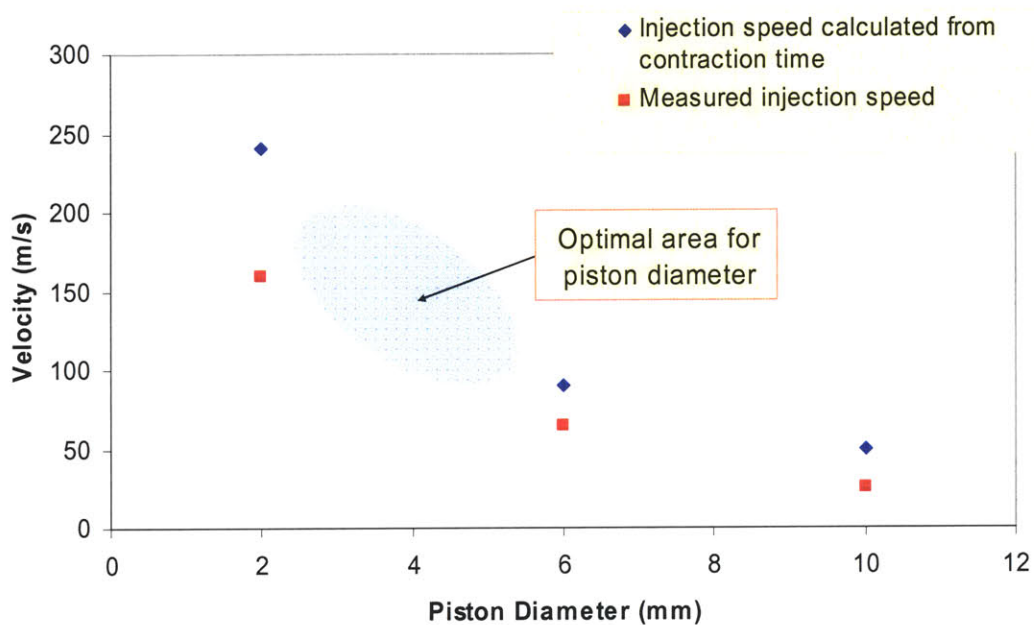


Figure 6-24. Optimal piston diameter for Prototype 2 design.

Table 6-6. Design parameters for drug vials from 3 mm to 5 mm.

Piston Diameter (mm)	Volume (μL)	Predicted Velocity (m/s)
3	42	200*
4	88	150*
5	137	100*

* Predicted speed from Figure 6-24

7 Conclusion

Prototypes 1 and 2 both achieved successful injection into pig skin. Injection depths varied inversely as a function of drug volume due. Depth penetration into the skin was found to be between 15 mm for the 20 μL drug volume and 1mm for the 200 μL drug volume. Drug volumes larger the 200 μL were unable to penetrate the skin because the required piston diameter was too large to yield the necessary injection pressure. It was clearly observed that successful injections are related to the drug speed. Drug speeds above 100 m/s with stream diameters of 100 μm penetrated the skin and faster drug rates penetrated deeper into the tissue. For the drug volumes used in Prototype 2, the drug speed ranged from 160 m/s to 25 m/s as the drug volume increased. The experiments showed that an optimal drug vial diameter for this setup lie between 3 mm and 5 mm yielding a drug volumes of 50 μl to 138 μL .

Power consumption during successful injections was approximately 60 J. Increasing the power dissipation with the use of larger capacitors did not result in a major increase in the injection velocity. This was possibly due to a strain rate limitation for the given pressure requirement.

Needle-less injection systems using NiTi actuator show promise as a viable product. Further research is needed to find the optimal design of many of the parameters. This thesis shows that a hand held device using NiTi actuation is capable of injection fluid to the necessary depths in animal tissue.

8 Further Research

8.1 Prototype 2

Prototype 2 provided valuable information about the drug speeds and penetration depth. From this data, the optimal drug vial diameter was obtained given a 100 μm orifice, 7.5mm contraction length and using 8 NiTi wires. Experiments on drug vials in the 3 mm to 5 mm range would verify this analysis.

Changes to Prototype 2's moving parts (the pusher, piston, and push block) could be made to decrease friction and lower the design's weight. These changes may decrease the force necessary to inject into skin.

Adding more NiTi wire to the device would provide more force for injection and may be useful if larger drug volumes are used.

Accurate measurements of energy dissipated should also be taken using a precision resistor in series with the NiTi to measure the current.

8.2 Strain rate measurements

An experiment to determine the strain rate as a function of load for NiTi could be conducted. This data could help in designing the optimal drug vial size by providing insight to explain why the 2 mm drug vial did not have a marked change in drug speed when more power was supplied. Such data could support the hypothesis that input energy-strain rate relationship plateaus in this design.

8.3 Further research prototypes

Once the ideal drug volume and piston diameter are found a hand-held injection device could be created as a further proof of concept. This device should have disposable drug vials and be fully self contained.

The drug vials should be designed in such a way as to be fully disposable and contain the piston, nozzle and orifice. The overall device should have an integrated power source.

References

1. Chan, W. Instrumentation to Characterize Needle Insertion into Biological Tissue [Master of Science Thesis]. Cambridge MA: MIT; 2002 June
2. Gere, J., Tomoshenko, S. Mechanics of Materials. 4thed., Boston Ma: PWS Publishing Company, 1997,pp556,889.
3. Lafontaine, S. Fast Shape Memory Alloy Actuators [Doctor of Philosophy Thesis]. Montréal Canada: McGill University; 1997 July
4. Ölander, A. Journal of the American Chemical Society, 1932 3819.
5. Sullivan, T., Eaglstine, W., Davis S., Mertz, P. The pig as a model for human wound healing. *Wound Repair and Regeneration*. Vol 9, No 2, pp.66-76.
6. White, F. M. Fluid Mechanics. 3rd ed., New York: McGraw-Hill.Inc,1994,pp.23.
7. Dynalloy, Inc. [Web Site]. <http://dynalloy.com>. 2003.
8. Extech Instruments Corporation. [Web Site]. <http://www.extech.com/>. 2003.
9. Injex [Web Site]. <http://www.equidyne.com/>. 2003.
10. MathCad [Web Site]. <http://www.mathcad.com/>. 2003.
11. Mediject VISION [Web Site]. <http://www.mediject.com/>. 2003.
12. Norwood Abbey, Inc. [Web Site]. <http://www.norwoodabbey.com/indexfl.htm>. 2003.
13. Penjet [Web Site]. <http://www.penjet.com>. 2003.

14. Powderject [Web Site]. <http://www.powderject.com>. 2003.
15. Shape Memory Applications, Inc. [Web Site]. <http://www.sma-inc.com/>. 2003.
16. Solidworks [Web Site]. <http://www.solidworks.com/>. 2003.
17. Tektronics [Web Site]. <http://www.tek.com/>. 2003.
18. Weston Medical [Web Site]. <http://www.weston-medical.com/>. 2003.

Appendix A

Feasibility Analysis

Pressure calculation for skin penetration

$$D_s := 100 \cdot 10^{-6} \text{ m}$$

$$F := .15 \text{ N}$$

Given Values
Calculated

$$A_{cc} := \left(\frac{D_s}{2} \right)^2 \cdot \pi$$

$$A_{cc} = 7.854 \times 10^{-9} \text{ m}^2$$

Cross-sectional area of drug stream

$$P := \frac{F}{A_{cc}}$$

$$P = 1.91 \times 10^7 \text{ Pa}$$

Local high pressure needed to penetrate the skin

Drug volume diameter

$$Vol := 200 \cdot 10^{-6} \text{ L}$$

$$L_c := 7.5 \cdot 10^{-3} \text{ m}$$

$$L_t := 150 \cdot 10^{-3} \text{ m}$$

$$D_{pl} := 2 \sqrt{\left(\frac{Vol}{L_c \cdot \pi} \right)}$$

$$D_{pl} = 5.827 \times 10^{-3} \text{ m}$$

Diameter of drug volume

$$P_{cc} := \frac{Vol}{L_c \cdot \pi}$$

$$P_{cc} = 8.488 \times 10^{-6} \text{ m}^2$$

Piston cross-sectional area

$$Freq := P \cdot \frac{Vol}{L_c \cdot \pi}$$

$$Freq = 162.114 \text{ N}$$

Force required by NiTi

Number of SMA wires

$$D_{sma} := 380 \cdot 10^{-6} \text{ m}$$

$$P_{sma} := 200 \cdot 10^6 \text{ Pa}$$

Drug volume and wire contraction

$$A_{sma} := \left(\frac{D_{sma}}{2} \right)^2 \cdot \pi$$

$$A_{sma} = 1.134 \times 10^{-7} \text{ m}^2$$

Cross-sectional area of NiTi wire

$$F_{sma} := A_{sma} \cdot P_{sma}$$

$$F_{sma} = 22.682 \text{ N}$$

Force available from NiTi

$$N := \frac{Freq}{F_{sma}}$$

$$N = 7.147$$

Number of NiTi wires

Contraction Speed

$$V_d := 100 \frac{\text{m}}{\text{s}}$$

Drug velocity

$$V_{lc} := V_d \cdot \frac{A_{cc}}{P_{cc}}$$

$$V_{lc} = 0.093 \frac{\text{m}}{\text{s}}$$

Velocity of contraction

$$\text{erate} := \frac{V_{lc}}{L_t}$$

$$\text{erate} = 0.617 \text{ Hz}$$

Strain rate required

Energy required for actuation

$$\varepsilon := .02$$

NiTi efficiency

$$E := \text{Freq} \cdot L_c$$

$$E = 1.216 \text{ J}$$

Energy required if %100 efficiency for NiTi

$$E_{\text{actual}} := \frac{E}{\varepsilon}$$

$$E_{\text{actual}} = 60.793 \text{ J}$$

Actual theoretical energy required for injection

Appendix B

Turbulent flow analysis

Given Parameters

Tube Diameter:

$$Dt := 100 \cdot 10^{-6} \text{ m}$$

Tube Length:

$$Lt := 500 \cdot 10^{-6} \text{ m}$$

Viscosity Fluid:

$$\mu := 1.3 \cdot 10^{-3} \frac{\text{N} \cdot \text{s}}{\text{m}^2}$$

Density Fluid

$$\rho := 998 \frac{\text{kg}}{\text{m}^3}$$

$$V := 140 \frac{\text{m}}{\text{s}}$$

$$\varepsilon := 1 \cdot 10^{-6} \text{ m}$$

$$g := 9.8 \frac{\text{m}}{\text{s}^2}$$

Reynolds Number

$$Re := \frac{(\rho \cdot Dt \cdot V)}{\mu} \quad Re = 1.075 \times 10^4$$

Turbulat Flow Friction Factor

$$\text{tran} := -1.8 \cdot \log \left[\left(\frac{6.9}{Re} \right) + \left(\frac{\varepsilon}{Dt} \right)^{1.11} \right]$$

$$f := \left(\frac{1}{\text{tran}} \right)^2 \quad f = 0.043$$

Pressure Drop in Tube

$$hf := f \cdot \frac{Lt \cdot V^2}{Dt \cdot 2g} \quad hf = 213.619 \text{ m}$$

$$\text{deltaP} := \rho \cdot g \cdot hf \quad \text{deltaP} = 2.089 \times 10^6 \text{ Pa}$$

Appendix C

Pressure drop around plunger

Given Parameters

Drug Specs

Injection Time	Volume of Drug	Viscosity Fluid:	Density Fluid	
$T := 80 \cdot 10^{-3} \text{ sec}$	$V_d := 200 \cdot 10^{-6} \text{ liter}$	$\mu := 1.3 \cdot 10^{-3} \frac{\text{N} \cdot \text{s}}{\text{m}^2}$	$\rho := 1000 \frac{\text{kg}}{\text{m}^3}$	$g := 9.8 \frac{\text{m}}{\text{s}^2}$

Plunger Specs

$D_{pl} := 5.95 \cdot 10^{-3} \text{ m}$	Diameter of Plunger rod
$l_{pl} := 60 \cdot 10^{-3} \text{ m}$	length of plunger rod
$D_{cyl} := 6.00 \cdot 10^{-3} \text{ m}$	Diameter of cylinder

$D_{gap} := \frac{(D_{cyl} - D_{pl})}{2}$	$D_{gap} = 2.5 \times 10^{-5} \text{ m}$	Thickness of gap
---	--	------------------

$A_{pl} := \pi \left(\frac{D_{pl}}{2} \right)^2$	$A_{pl} = 2.781 \times 10^{-5} \text{ m}^2$	Area of Plunger
---	---	-----------------

$A_{cyl} := \pi \left(\frac{D_{cyl}}{2} \right)^2$	$A_{cyl} = 2.827 \times 10^{-5} \text{ m}^2$	Area of Cylinder
---	--	------------------

$A_{gap} := A_{cyl} - A_{pl}$	$A_{gap} = 4.693 \times 10^{-7} \text{ m}^2$	Area of Gap
-------------------------------	--	-------------

Flow Calc

$Q_{dot} := \frac{V_d}{T}$	$Q_{dot} = 2.5 \times 10^{-6} \frac{\text{m}^3}{\text{s}}$
----------------------------	--

$v_{drug} := \frac{Q_{dot}}{A_{gap}}$	$v_{drug} = 5.327 \frac{\text{m}}{\text{s}}$	Velocity of Drug
---------------------------------------	--	------------------

$D_h := 4 \cdot \frac{A_{gap}}{2(\pi D_{cyl}) + 2 \cdot D_{gap}}$		Hydrolic Diameter
---	--	-------------------

$Re := \frac{(\rho \cdot D_{gap} \cdot v_{drug})}{\mu}$	$Re = 102.449$	Reynolds Number
---	----------------	-----------------

$f := \frac{96}{Re}$	$f = 0.937$	Friction Factor
----------------------	-------------	-----------------

$$hf := f \cdot \frac{Plen \cdot Vdrug^2}{Dgap \cdot 2g}$$

Head thign

$$\text{deltaP} := \rho \cdot g \cdot hf$$

Pressure Drop across the plunger

$$\text{deltaP} = 3.191 \times 10^7 \text{ Pa}$$

Hoop Stress calculations

Hoop stress in cylinder due to pressure of injection

$$P := 1.91 \cdot 10^7 \text{ Pa} \quad \text{Pressure during injection}$$

$$\sigma_y := 30 \cdot 10^6 \text{ Pa} \quad \text{Yield stress for aluminum alloys (low estimate)}$$

$$D := 6 \cdot 10^{-3} \text{ m} \quad \text{Cylinder diameter}$$

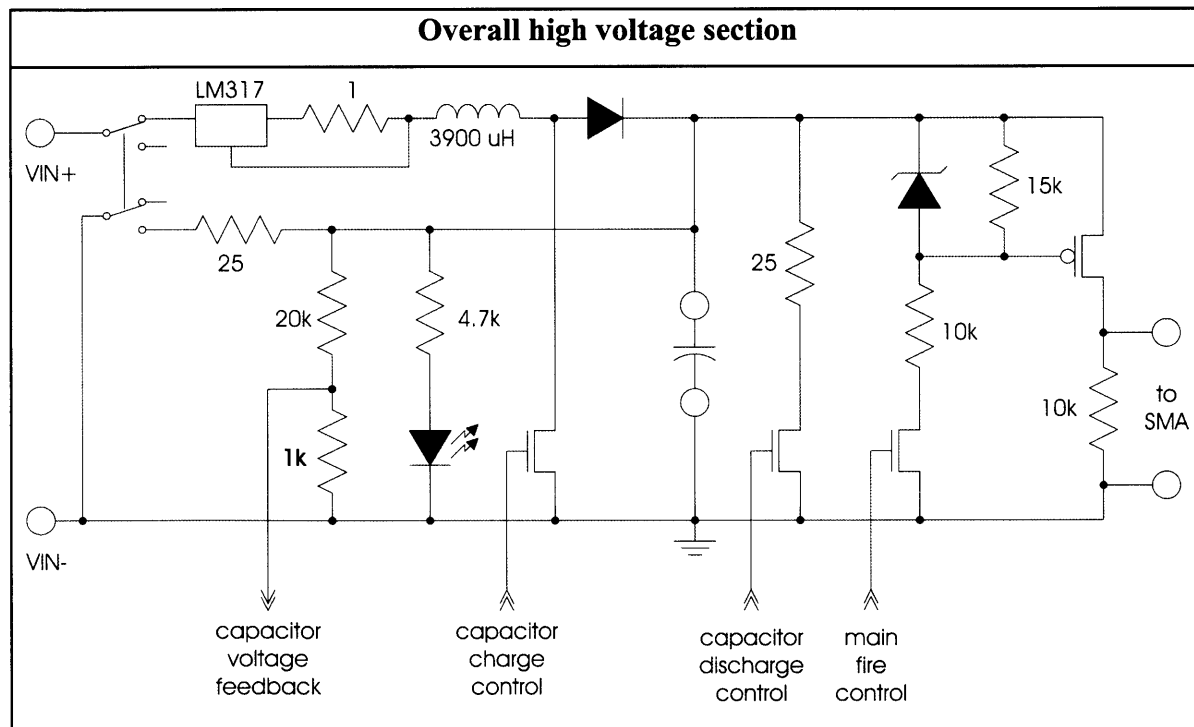
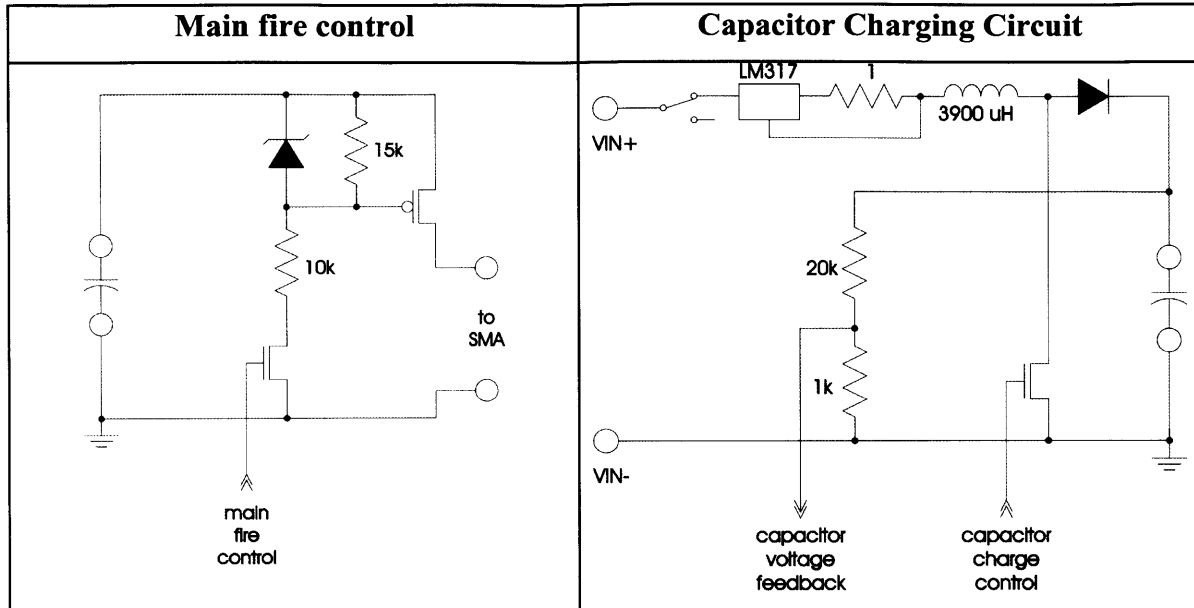
$$t := P \cdot \left(\frac{D}{2 \cdot \sigma_y} \right) \quad \text{Hoop strength}$$

$$t = 1.91 \times 10^{-3} \text{ m} \quad \text{Minumum thickness to insure no}$$

The minimum wall thickness was determined to be 2mm. A wall thickness of 4.5mm was chosen as for Prototype 1.

Appendix D

Power supply circuit

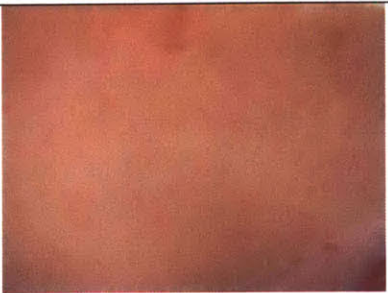
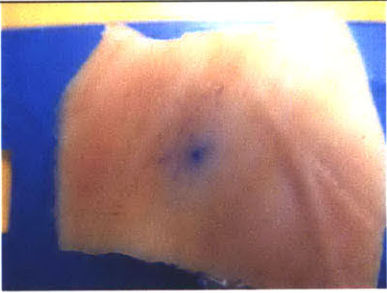
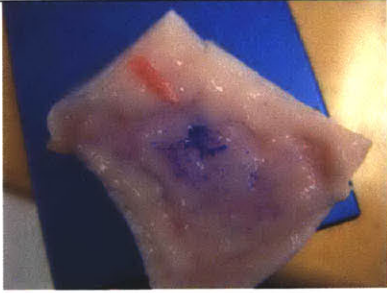




***This circuit was designed by Johann Burgert and Jan Malásek**




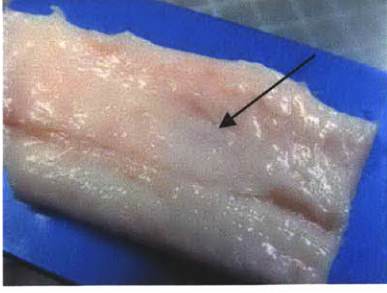

Appendix E

Prototype 2 injection photographs

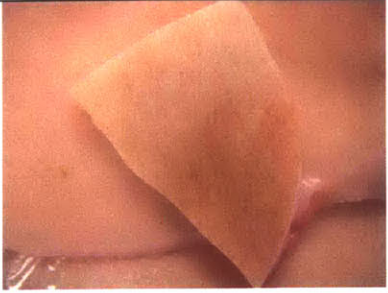
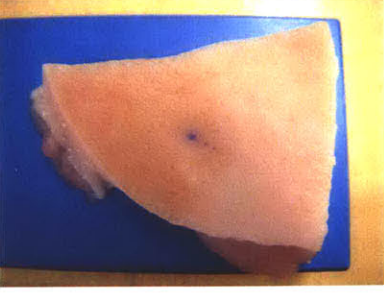
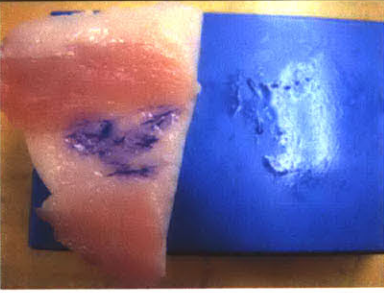

2 mm drug vial

View	Before injection	After injection
Front		
Back	none	
Section		






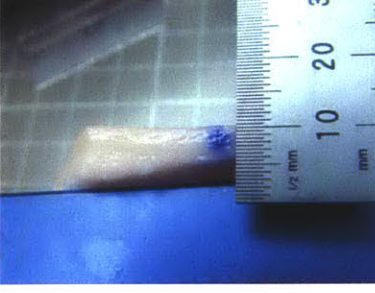
2 mm drug vial

View	Before injection	After injection
Front	 A close-up photograph of a person's skin before an injection. The skin is light-colored and appears slightly taut.	 A photograph of the skin after an injection. A small, faint blue mark is visible on the skin surface. The skin is resting on a blue surface.
Back	 A close-up photograph of a person's skin before an injection. The skin is light-colored and appears slightly taut.	 A photograph of the skin after an injection. A small, faint blue mark is visible on the skin surface, indicated by a black arrow. The skin is resting on a blue surface.
Section	none	 A photograph of a skin section. A ruler is placed next to the skin for scale. The ruler shows markings in millimeters (mm) and half-millimeters (1/2 mm). The skin section is approximately 10 mm long. A small blue mark is visible on the skin surface.

2 mm drug vial

View	Before injection	After injection
Front		
Back	none	
Section	none	

2 mm drug vial

View	Before injection	After injection
Front	 A close-up photograph of the front of a 2 mm drug vial. The vial is a translucent, cylindrical tube with a slightly wider base. It is held against a light-colored, possibly skin, background.	 A close-up photograph of the front of the 2 mm drug vial after injection. A small, dark blue spot is visible on the surface of the vial, indicating the injection site.
Back	 A close-up photograph of the back of the 2 mm drug vial before injection. The vial is held against a light-colored background.	 A close-up photograph of the back of the 2 mm drug vial after injection. A dark blue spot is visible on the back of the vial, indicating the injection site.
Section	 A close-up photograph showing a cross-section of the 2 mm drug vial before injection. The vial is held against a light-colored background.	 A close-up photograph showing a cross-section of the 2 mm drug vial after injection. A dark blue spot is visible on the surface of the vial. A ruler is placed next to the vial for scale, showing markings in millimeters (mm) and half-millimeters (1/2 mm).